electronics

MDPI

Review

Overview of Signal Processing and Machine Learning for Smart Grid Condition Monitoring

Elhoussin Elbouchikhi [1,*], Muhammad Fahad Zia [2,3], Mohamed Benbouzid [3,4] and Soumia El Hani [5]

1 ISEN Yncréa Ouest, LABISEN, Rue Cuirassé Bretagne, 29200 Brest, France
2 Department of Electrical Engineering, National University of Computer and Emerging Sciences, Lahore 54000, Pakistan; fahad.zia@nu.edu.pk
3 Institut de Recherche Dupuy de Lôme (UMR CNRS 6027 IRDL), University of Brest, 29238 Brest, France; mohamed.benbouzid@univ-brest.fr
4 Logistics Engineering College, Shanghai Maritime University, Shanghai 201306, China
5 "Energy Optimization, Diagnosis and Control" Research Group, STIS Research Center, Mohamed V University, ENSAM, Rabat 10100, Morocco; s.elhani@um5r.ac.ma
* Correspondence: elhoussin.elbouchikhi@isen-ouest.yncrea.fr

Abstract: Nowadays, the main grid is facing several challenges related to the integration of renewable energy resources, deployment of grid-level energy storage devices, deployment of new usages such as the electric vehicle, massive usage of power electronic devices at different electric grid stages and the inter-connection with microgrids and prosumers. To deal with these challenges, the concept of a smart, fault-tolerant, and self-healing power grid has emerged in the last few decades to move towards a more resilient and efficient global electrical network. The smart grid concept implies a bi-directional flow of power and information between all key energy players and requires smart information technologies, smart sensors, and low-latency communication devices. Moreover, with the increasing constraints, the power grid is subjected to several disturbances, which can evolve to a fault and, in some rare circumstances, to catastrophic failure. These disturbances include wiring issues, grounding, switching transients, load variations, and harmonics generation. These aspects justify the need for real-time condition monitoring of the power grid and its subsystems and the implementation of predictive maintenance tools. Hence, researchers in industry and academia are developing and implementing power systems monitoring approaches allowing pervasive and effective communication, fault diagnosis, disturbance classification and root cause identification. Specifically, a focus is placed on power quality monitoring using advanced signal processing and machine learning approaches for disturbances characterization. Even though this review paper is not exhaustive, it can be considered as a valuable guide for researchers and engineers who are interested in signal processing approaches and machine learning techniques for power system monitoring and grid-disturbance classification purposes.

Keywords: smart grid; resilience; signal processing; disturbance classification; power quality; PSD estimation; demodulation methods; time-frequency analysis; pattern recognition techniques; machine learning; information theoretical criteria

Citation: Elbouchikhi, E.; Zia, M.F.; Benbouzid, M.; El Hani, S. Overview of Signal Processing and Machine Learning for Smart Grid Condition Monitoring. *Electronics* **2021**, *10*, 2725. https://doi.org/10.3390/electronics10212725

Academic Editors: Ahmed F. Zobaa and Giambattista Gruosso

Received: 29 August 2021
Accepted: 6 October 2021
Published: 8 November 2021

1. Introduction

A smart grid is a developing electrical network of transmission lines, switches and transformers, protection equipment, sensors, computers, automations, controls and new communication and information technologies working together in order to meet the 21st century demand for electricity while reducing greenhouse gas emissions and handling the security and privacy issues [1–3]. It is characterized by a two-way dialogue where electricity and information can be exchanged between the utility grid, microgrids and its costumers and aggregators [4]. This two-way exchange makes the electrical grid more efficient, more reliable, more secure, and greener. A smart grid enables newer technologies

to be integrated such as solar panels, wind turbines, marine renewable energy resources, plug-in electric vehicle charging, and green hydrogen production through electrolysis of water, etc. [5–7]. Moreover, the smart grid will enable power system operators to control and manage the electricity demand with the cooperation of customers especially during peak power demand times [8]. This implies the need for smart-meters and smart-appliances to be implemented at houses and buildings level using the Internet of Things (IoT) concept for demand response management [9–11]. As a result, utilities will achieve an operating cost reduction by shifting electricity usage away from peak hours and having appliances and devices running during off-peak periods. Consequently, electricity production is more evenly distributed throughout the day, which mitigates electric grid congestion. Smart grid technologies provide a huge amount of relevant information that enables grid operators to supervise and manage the electricity demand in real-time, which reduces outages, lowers the need for peak power facilities, and allows operators to predictably manage electricity production [12,13].

Traditionally, utilities typically rely on complex power distribution schemes and manual switching to ensure power flow to the customers. Any breakage in the distribution network caused by storms, bad weather or sudden changes in the electricity demand can lead to outages. The smart grid distribution intelligence counters these energy fluctuations and outages by automatically identifying problems and actuating backup facilities (conventional power plants, storage systems, distributed energy generation, etc.) or shedding non-critical loads using demand response incentives in order to ensure the continuity of power delivery [14,15]. In the near future, the main grid is expected to experience a significant mutation in order to be cost-effective, self-healing, and resilient to system anomalies while meeting power quality standards [16–18].

Power quality (PQ) focuses on the interaction between the power grid and the end-users and involves both voltage and current quality [19,20]. Voltage quality measures the way the power system affects the customers and their appliances, and current quality measures the way the end-users loads affect the grid [21]. Power system voltage deviations from nominal values are considered as disturbances, which can be categorized into two classes: power quality deviation and events. Power quality deviation includes small variations of voltage and frequency around their nominal values. Events, however, stand for large deviations from nominal values and include mainly voltage sag and voltage swell, which may lead to power supply interruption. Other disturbances can effect the power quality such as flicker, harmonics and interharmonics [22,23]. These disturbances can have a huge impact over power delivery reliability, metering performance, equipment lifespan, and may lead to protection devices malfunctioning and big issues of electromagnetic compatibility. Consequently, power quality monitoring is of paramount importance in smart grids [24–26].

Within this context, power quality has become essential for building the future smart grid. Control, energy management, and condition monitoring of power systems is mandatory in order to increase its reliability and availability and reduce outages and shut-downs in future smart grids [27,28]. A wide area measurement system (WAMS) is a set of advanced measurement devices, information and communication technologies, and operational infrastructure that enhance the situational awareness of the grid operator. WAMS helps trigger a proactive power quality disturbance detection, which allows activating a fault ride-through approach, minimizing downtime, and operating and maintenance costs while maximizing productivity [29]. Phasor Measurement Units (PMU) is a key component of WAMS that plays a key role in supervising and identifying the operating state of the smart grid by collecting and processing electrical signals (currents and voltages) [30]. The IEC/IEEE 60255-118-1 standard divides PMUs into P-class and M-class PMUs [31]. It is defined as a device used to estimate the magnitude and phase angle of an electrical phasor quantity (such as voltage and current) in the electric grid using a common time source for synchronization. These measurements are critical because if the grid supply/demand balance is not perfectly matched, frequency imbalances and voltage amplitude fluctuations

can cause stress on the grid, which is a potential cause of power outages [32]. It is worth emphasizing that optimal PMU placement in WAMS is one of the most investigated issues by researchers and engineers in order to improve the observability and security of the power system [33,34].

The last few years have witnessed the publication of several original papers, reviews, and survey papers dealing with the timely topic of transmission and distribution networks condition monitoring, and microgrids and smart grids resilience. Table 1 provides the main published review papers and their contributions. Various signal processing techniques have been extensively investigated for disturbance features extraction in PMUs. Indeed, several approaches have been proposed in the literature such as the Interpolated Discrete Fourier Transform (IpDFT) and its extensions [35], the Taylor Weighted Least-Squares (TWLS) [36], the Kalman filter [37], and the Frequency Down-Conversion and Low-Pass Filtering (DCF) technique [38]. Moreover, adaptive extended Kalman filter has been proposed for achieving better phasor and frequency estimations of PMUs under changing harmonics [39]. The Clarke transformation-based DFT method was proposed for attaining better accuracy of phasor and frequency estimations [40]. A quasipositive-sequence DFT method has been proposed for single phase angle estimation in [41]. A modified DFT method was presented to accurately obtain a phasor estimate in the presence of a decaying DC offset in [42]. Moreover, an iterative IpDFT method has also been proposed for synchrophasor estimation under static conditions in [43]. Interpolated dynamic DFT (IpD2FT) has been proposed for obtaining superior estimation of dynamic frequency and synchrophasor in [44]. Similarly, double suboptimal-scaling-factor adaptive strong tracking Kalman filter has been used to achieve better accuracy in dynamic phase estimation under transient conditions [45]. The accuracy of dynamic phasor estimation had also been improved by using Gauss-Newton ADALINE [46] and Taylor K-Kalman filters [47]. In an unbalanced three-phase power system, frequency estimation has been improved by a coupled orthogonal constant modulus algorithm [48]. In [49], a modular positive-sequence estimation algorithm was presented to achieve better accuracy of synchrophasor estimation. Amplitude and phase modulation models of the signal have been used for better dynamic phasor estimation under off-nominal frequency and oscillations conditions [50]. An empirical wavelet transform method was also developed for obtaining phasor estimation at the distribution level [51]. In [52], a compressive sensing-based Taylor-Fourier method was developed for achieving multi-frequency phasor estimation in distribution systems. A sync interpolation function has been used to improve dynamic synchrophasor estimation in [53]. A low-complexity weighted least square method has also been proposed to improve phasor and frequency estimations of power systems under off-nominal operating conditions [54]. In [55], the accuracy of dynamic phase estimation was improved using a combination of Taylor weighted least squares and matrix pencil method against an out-of-band interference compromised signal. Furthermore, a weighted Taylor-Fourier transform was also developed to achieve better synchrophasor estimation with low computational complexity in [56].

Table 1. A list of review papers dealing with power systems monitoring.

Year	Ref.	Contributions
2015	[57]	This paper provides a comprehensive review of digital signal processing and machine learning techniques for automatic classification of power quality (PQ) events by investigating the effect of noise on these approaches' performance.
2017	[58]	This paper reviews smart grid features and data issued from various energy resources and discusses techniques used for big data analysis in smart grid applications.
2019	[59]	This article provides a comprehensive review on digital signal processing (DSP) methods for fault detection and machine learning for fault classification and causes identification. The focus is to provide an overview of techniques used for automatic recognition of PQ events. Specifically, microgrid applications have been considered where the use of power electronic technology in renewable energy systems and distributed generators increases the risk of PQ issues.
	[60]	This paper reviews machine learning and big data techniques for efficiently processing the massive data volume generated by Internet of Things (IoT) devices for reliable decision-making and ensuring the safety of both data and infrastructure against cyber attacks in a smart grid.
2020	[61]	This paper presents failures in smart grid components (conventional energy systems, renewable resources, cables and transmission lines, power electronics and power transformers) and describes sensors, communication tools, including 5G, and monitoring infrastructure. Moreover, it discusses procedures associated with smart grids fault detection and location and provides an insight into lessons learned and future trends.
	[62]	This paper reviews signal processing techniques and machine learning approaches used in the field of power quality disturbance detection and classification.
	[63]	This review paper highlights the interest of machine learning techniques for the efficient handling of a massive amount of data generated from smart meters and phasor measurement units in the next generation of power systems.
	[64]	This paper provides a critical review of approaches used for PQ disturbances detection and classification in the utility grid with renewable energy integration. It presents various concepts utilized for features extraction for detecting and classifying PQ disturbances in a noisy environment.

In this context, this paper focuses on power quality monitoring in a smart grid. The main objective is to present a state-of-the-art review on the methods, advances and prospects on signal processing for feature extraction [23,65] and pattern recognition techniques for electric power grid monitoring and disturbance classification [59,66,67]. To this end, power spectral density estimation techniques, which are termed frequency-domain algorithms, are first presented to deal with stationary signals, which are more appropriate for steady state conditions [68]. Classical methods are presented and critically analyzed, then more advanced power spectral density estimation approaches are discussed such as Maximum Likelihood estimation (MLE), Multiple Signal Classification (MUSIC), Estimation of Signal Parameters via Rotational Invariance Techniques (ESPRIT) and AutoRegressive Moving Average (ARMA) techniques [69–71]. Afterward, demodulation techniques, which are considered as time-domain algorithms, are explored for instantaneous frequency and instantaneous amplitude tracking. The aforementioned approaches present the interest of being easy to implement but assumes the signal to be mono-component; a sinusoid, which may be amplitude and/or frequency modulated [72,73]. For multi-component signals, a filtering approach is first required to separate the frequency components (modes) before applying the appropriate demodulation technique. In the case where mono-component signals can not be extracted by filtering, more sophisticated approaches are required such as Empirical Mode Decomposition (EMD) [74] and its extensions or Discrete Wavelet transform (DWT) [75–77]. For transient and nonstationary environments, time-frequency and time-scale approaches are more appropriate and are extensively discussed in this paper [78–80]. These approaches allow retrieving the evolution of signal frequency content and amplitudes over time and allow abnormal operating condition tracking over time. Generally speaking, all the previously discussed methods for PQ monitoring try to deal

with the trade-off between frequency estimates accuracy and reporting latency, which is related to the computational burden of the method, especially in P-class PMUs [81,82].

These signal processing approaches allow signal feature extraction. For the results to be analyzed and interpreted, an expert of power systems and power quality monitoring is required, and in some conditions, the results analysis is quite complicated. To perform an automatic detection, power quality disturbances classification and decision making, it is mandatory to implement sophisticated artificial intelligence techniques. Hence, for the sake of power quality disturbances classification, some classical classifiers are used such as the ABC classifier [83] and symmetrical component classifier [84]. Moreover, pattern recognition techniques have been extensively investigated in the literature for power systems monitoring such as Artificial Neural Network (ANN), Support Vector Machine (SVM), etc. [85–93]. Furthermore, deep learning algorithms have the inherent capability to automatically learn optimal features from raw input data, without pre-processing using sophisticated signal processing techniques. These approaches include and are not limited to convolution neural network (CNN), recurrent neural network (RNN), identity-recurrent neural network (I-RNN), long short-term memory (LSTM), gated recurrent units (GRU) and convolutional neural network-long short-term memory (CNN-LSTM). These approaches have not only been proposed for power quality disturbances classification but also for power system protection [94], renewable energy forecasting and energy production prediction [95] as well as consumer profile identification and uncertainty management [96]. In addition to that, information criteria rules and detection theory have been proposed and their efficiency has been proven to overcome the complexity and the computational burden of AI techniques [97].

The main contributions of the paper are threefold:

- A systematic review of smart grid disturbances, PMU requirements for PQ measurement, and European and international PQ standards is presented,
- An in-depth and comprehensive survey of methods for grid frequency, rate of change of frequency (ROCOF) and synchronized phasor estimation is provided.
- A survey on classification methods for intelligent system application to disturbances diagnosis in power systems is conducted. A critical analysis on signal processing and machine learning is presented and a brief discussion on relevant topics for future developments is conducted.

The remainder of the paper is organized as follows. Section 2 presents the main power quality disturbances reported in the literature. Then, it deals with the power quality measurement issue and presents the phasor measurements units implemented in critical power system substations for condition monitoring. Section 3 presents major advances in signal processing techniques for frequency and phasor estimations for electric power grid monitoring. Then, Section 4 briefly describes some major classification and pattern recognition techniques for disturbances classification and root causes identification. Finally, conclusions and future challenges regarding power system monitoring are provided in Section 5.

2. Power Quality Measurement

Over the last decades, there has been a significant increase in the use of the nonlinear loads consisting of power electronics converters in power networks. The use of such systems can induce harmonic pollution, disturbances, and power quality events within a power grid, leading to abnormal operating conditions of equipment and materials. It is, therefore, mandatory to characterize power quality disturbances in order to enhance the power system's efficiency and reliability [97,98].

2.1. Power Grid Disturbances

Power grid disturbances can be classified as either affecting the fundamental frequency component (50 Hz or 60 Hz) or harmonic disturbances. Fundamental frequency disturbances affect the amplitude, frequency, and initial phase shift of the fundamental frequency

such as voltage dips, outages, overvoltages and unbalances. Harmonic disturbances induce distortion of the signals (voltages or currents) waveform and are characterized by the appearance of new frequency components that are multiples of the fundamental frequency.

2.1.1. Typical Power Quality Disturbances

A balanced electrical grid is a three-phase power system characterized by sinusoidal waveforms, where the three-phases have the same fundamental frequency (equal to the nominal value), the same voltage magnitude, and a phase shift of 120°. If one of these conditions is not satisfied, the power grid is considered to be experiencing a power quality disturbance. A power quality disturbance is defined as any problem that causes voltage or frequency deviations in the power supply and may result in equipment failure or malfunction of the power grid, which may cause issues at the load ends. These power quality events include voltage sag, very short interruptions, voltage swell, voltage fluctuation, voltage unbalance, harmonics, inter-harmonics, distortion, spikes, notches, flicker, noise and transients. Figure 1 depicts a classification of major power quality disturbances as described in the literature [99–102]. These power quality disturbances can be broadly classified into two categories, which are power quality variations and events. Power quality variation is regarded as a steady-state disturbance and corresponds to a small frequency and amplitude deviation from its nominal values. Conversely, a power quality event is related to a large deviation such as outage, sag, and swell. These disturbances can have a substantial influence on grid stability, security (protective relays malfunction), equipment's useful life, and power system measurement performance and generate electromagnetic noise.

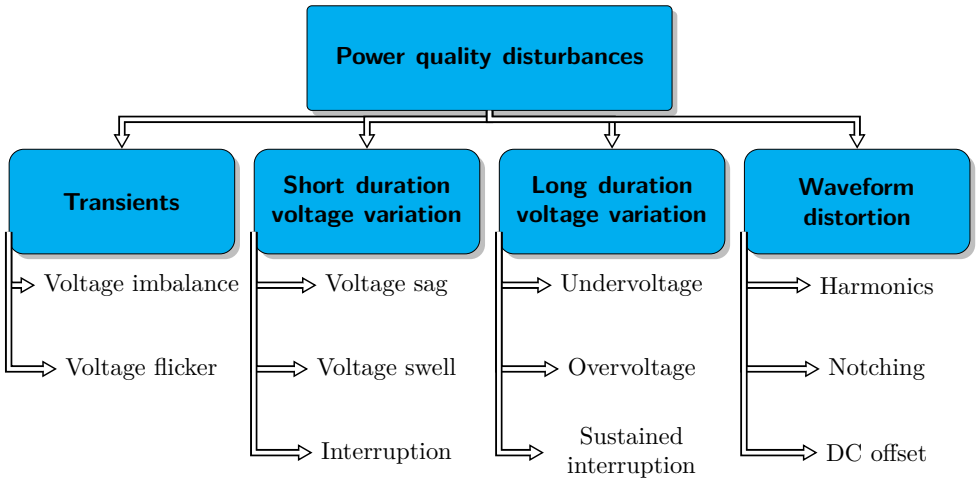

Figure 1. Power quality disturbance classification.

2.1.2. Causes and Consequences

Poor power quality issues can be due to several causes and conditions. Inductive and capacitive loads such as motors, ballasts, and electronic devices can induce a voltage and current phase angle, which deteriorates the power factor quality. Nonlinear loads and operating loads with rapidly changing energy demand cause harmonics, which require static and dynamic filters to mitigate. Improper load distribution across each phase leads to phases being unbalanced. High energy loads turning on or off cause voltage variations (dips and swells), which can be mitigated by proper load capacity resizing and adjusting transformer tapping. Transients are characterized by fast (sub-half cycle) changes in voltage, which exceeds the device insulation breakdown voltage rating, and are caused by switch contacts (arcing) and lightning.

These PQ disturbances affect businesses in different ways such as loss of production, products damage, reduced lifetime of equipment, loss of data or data corruption, etc. Table 2 summarizes typical power quality disturbance causes and the main consequences [99,103].

Table 2. Power quality disturbance causes and consequences.

Category	Typical Causes	Main Consequences
Notching	Lightning strike, transformer energization, capacitor switching, disconnection of heavy loads, power electronic rectifiers commutation	Destruction of components and insulation materials, data processing error, electromagnetic interference, etc.
Voltage spikes	Lightning, switching of lines or power factor correction capacitors, disconnection of heavy loads	Destruction of components and of insulation materials, data processing errors or data loss, electromagnetic interference
Voltage flicker	Line, capacitor or load switching, frequent start/stop of electric motors and oscillating loads, arc furnace	Light flickering, unsteadiness of visual perception
Overvoltage	Switching large load, energizing a capacitor bank, incorrect tap settings on transformers	Light flicker, stoppage or damage of sensitive equipment
Harmonic	Nonlinear loads (variable speed drives, SMPS), data processing equipment, high efficiency lighting, arc furnaces, electric machines working above the knee of the magnetization curve	Transformers overheating, neutral overload, overheating of cables and equipment, loss of efficiency in electric machines, increased probability in the occurrence of resonance, electromagnetic interference with communication systems, errors in measures when using average reading meters, nuisance tripping of thermal protections.
Undervoltage	Switching on a large load or switching off a large capacitor bank	Light flicker, unsteadiness of visual perception
Voltage swell	Start or stop of heavy loads, badly dimensioned power sources and regulated transformers, system faults, load and capacitor switching	Light flicker, data loss, stoppage or damage of sensitive equipment
Voltage sag	Faulty consumer installations, faulty transmission or distribution electric network, start-up of large motors and connection of heavy loads	Malfunction of information technology equipment, tripping of contactors and electromechanical relays and loss of efficiency in electric rotating machines
Interruptions	Equipment failure in the power system network, tripping of protection devices, storms, human errors, failure of protection devices	Stoppage of all equipment

Power quality characterization is of paramount importance in order to improve the power systems safety and reliability. Figure 2 depicts power quality characterization stages, which include signal acquisition based on appropriate sensors, feature extraction stage for signal parameter estimation, detection stage, and finally the classification stage to determine PQ disturbance types [104]. The feature extraction stage is performed based on advanced signal processing approaches, which include power spectral density estimation techniques, demodulation techniques, and time–frequency analysis. The classification stage is mainly performed using machine learning approaches.

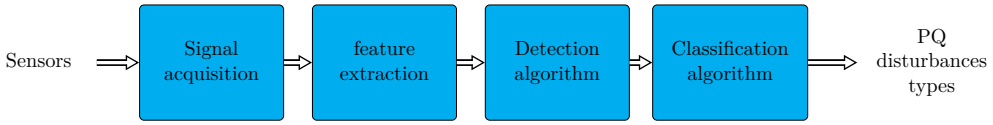

Figure 2. PQ monitoring algorithm.

2.2. Power Quality Analysis

Moving towards smart grids requires advanced control strategies, energy management systems, modern protective devices, and power quality monitoring to deal with PQ issues. The latter can be performed using measurement substations, which use intelligent electronic devices, including PMUs and supervisory control and data acquisition (SCADA)

infrastructure. PMUs are used for the secure measurement and parameter estimation of power signals. These parameters are transferred to a central controller via a SCADA infrastructure for further post-processing and transient characterization of PQ disturbance. These characteristics allow higher power quality and less downtime while supporting power from intermittent power sources and distributed generation.

2.2.1. Definition

Power quality is an estimate of the stability of the power supply in terms of voltage magnitude, frequency, and waveform required for the safe, correct, and continuous operation of a specific electrical load. Indeed, maintaining PQ requirements of voltage and current in a power system to the right level enables safe and continuous operation of electric loads. Good power quality can be viewed as a steady supply voltage that is within the prescribed range, has a frequency close to the rated value, and has a waveform close to sine wave (no distortion, no harmonics, no spikes and flicker, etc.). The electric power system is composed of electricity generation devices, electric power transmission lines, an electric power distribution network, and finally, the electricity meters at the end-users level. The electric power system complexity combined with meteorological events, generation and consumption fluctuations, power electronics usage at grid and consumers levels, as well as the integration of intermittent and distributed generation systems provide several factors that comprimise the power quality.

2.2.2. Wide Area Measurement System

A wide area measurement system (WAMS) is a stand-alone measurement technology, information tool, and operational infrastructure that complements the conventional supervisory control and data acquisition system (SCADA) used for main grid control and monitoring [34]. WAMS is designed for the monitoring of real-time dynamics of power systems, identification of control and stability weaknesses, and implementation of countermeasures in order to enhance the power system reliability [33]. It allows obtaining more detailed data (specifically, the real-time synchrophasors) on the steady-state power system operating condition and transients that arise due to various power system disturbances. The main objectives of WAMS are real-time monitoring, post-disturbance analysis, adaptive protection and power system restoration. Figure 3 provides a scheme describing the components of WAMS. It includes PMUs, PDC, GPS for time synchronization of the phasors, communication channels, visualization and analysis tools, a wide area situational awareness system and a wide area protection and control system.

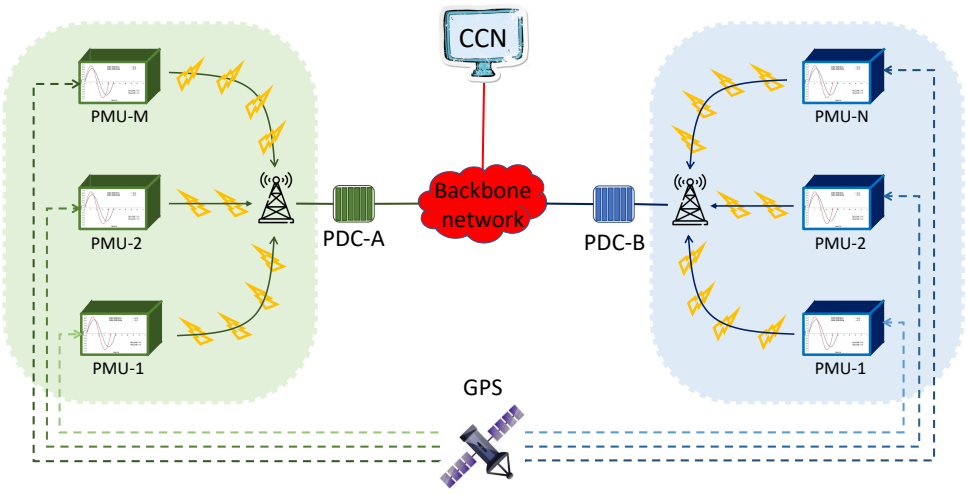

Figure 3. Phasor data concentrator in Wide Area Measurement System (CCN stands for central control network).

2.2.3. Phasor Measurement Units

A phasor measurement unit (PMU) is a high-speed smartmeter used for power systems state estimation and power quality monitoring with accuracy in the order of microseconds, which is much faster than the existing SCADA technologies [105,106]. PMU allows estimating the frequency, magnitude and phase angle of an electrical phasor quantity (voltage or current) with respect to global time reference in order to obtain synchronized real-time measurements of multiple widely dispersed locations in the power system network [107,108]. Time synchronization is mainly provided by the Global Positioning System (GPS) or IEEE 1588 Precision Time Protocol. The measured quantities are represented by a synchrophasor, as depicted by Figure 4. The calculation of real-time phasor measurements that are synchronized to an absolute time reference is of paramount importance as it allows an efficient response to power system disturbances and possible cascading blackouts.

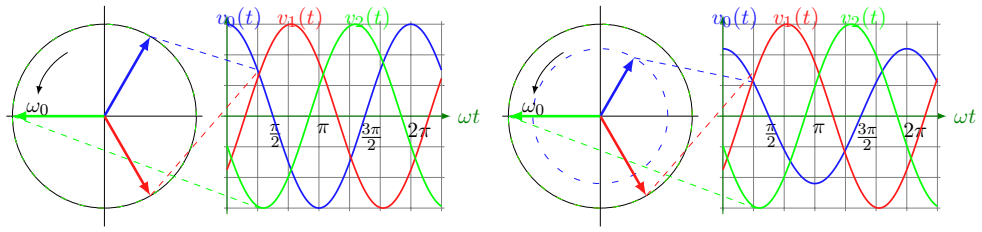

(a) Nominal condition. **(b)** Abnormal condition (voltage sag).

Figure 4. Synchrophasor representation of a sinusoidal signal for healthy and faulty conditions (voltage sag on phase 1).

PMU measures voltages and currents at critical substations of the power transmission lines and computes time-stamped phasors, as depicted by Figure 5. A real-time comparison of these synchronized measurements allows assessing power system conditions and detecting disturbances that may affect the power quality. The phasor data are collected either on-site or at centralized locations using Phasor Data Concentrator (PDC) technologies (see Figure 3) [109]. A PDC receives and time-synchronizes phasor data from multiple PMUs to produce a real-time, time-aligned output data stream. These data are then transmitted to a regional monitoring system (central control network), which is operated by the local grid operator. Due to the precise synchronization of the measurements, this power grid monitoring allows controlling power flow from multiple energy generation sources, implementing demand response mechanisms (load shedding) and event detection and classification for black-out event prevention [107].

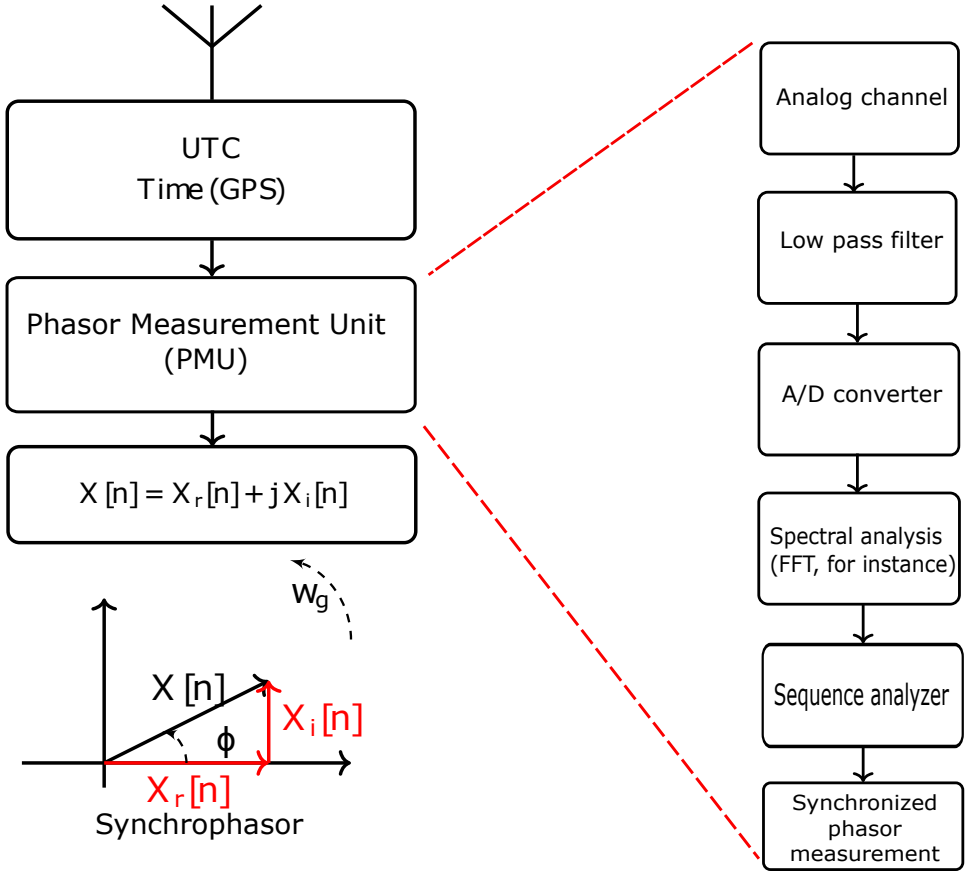

Figure 5. Phasor measurement units.

2.2.4. International Standards

Power quality in smart grids is defined by international standards and their local derivatives, adopted by various countries and electricity suppliers. Specifically, there are two international organizations that set forth power quality standards, which are the International Electrotechnical Commission (IEC) and the Institute of Electrical and Electronics Engineers (IEEE). Main power quality standards are as follows:

- IEC/IEEE 60255-118-1:2018 is used for synchrophasor measurement systems in power systems. It defines PMU, synchrophasor, frequency, and ROCOF measurements. Even though it does not provide hardware and software for computing these quantities, it specifies methods for evaluating the compliance of these measurements with standard requirements under both static and dynamic conditions.
- EN50160 is the European standard for power quality measurement, defining the acceptable limits of voltages and currents RMS values with respect to nominal values and the disturbance duration in AC power.
- IEEE-519 is the North American guideline for power systems. It is intended as "recommended practice" and refers to both current and voltage distortion.
- IEC 61000-4-30 is the standard defining methods for power quality monitoring. Specifically, it provides a description of measurement methods and PQ parameters interpretation [17]. Unlike earlier editions, the 2015 Edition 3 includes current measurements as well as voltage measurement.

Regarding PMU, the standard IEEE C37.118-2005 deals with issues related to PMUs integration into electric power systems. This standard is mainly describing the measurement accuracy testing and certification requirements, data transmission format and communication protocol. To handle power system dynamic behavior, the standard has been updated and split into two parts in 2011 (and its amendment C37.118-2014): C37.118-1 dealing with

the phasor estimation and C37.118-2 describing the communications protocol. Moreover, two PMU classes have been introduced: M class to use in steady state measurement and P class to track power system dynamic activity. The phasor measurement unit is intended for accurate phasor estimation under both steady state and dynamic conditions. To be compliant with the IEEE C37.118-2014 standard, the PMU measurement and estimation accuracy is measured through several parameters such as total vector error (TVE), frequency error, and rate of change of frequency error.

3. Grid Frequency and Phasor Estimation

In transmission and distribution grids, current and voltage waveform can be mathematically expressed as follows:

$$x[n] = a[n]\cos[\Phi[n]] + b[n] \tag{1}$$

where:

- $a[n]$ is the instantaneous amplitude,
- $\Phi[n] = 2\pi f_0[n]n + \varphi[n]$ is the instantaneous phase. $f_0[n]$ denotes the normalized instantaenous fundamental frequency and $\varphi[n]$ corresponds to the initial phase.
- $b[n]$ includes all possible disturbances, such as harmonics, inter-harmonics, and wideband noise.

In the following, commonly used approaches for PQ monitoring in PMUs are presented. Specifically, the focus is made on conventional approaches for static and dynamic conditions and power spectral density estimation for stationary signals analysis. Then, demodulation techniques and time–frequency representations are discussed and critically reviewed. These methods allow fault feature extraction based on PMU measurements. The challenge, then, is accurately estimating fundamental frequency $f_0[n]$, ROCOF using the first- and second-order backward Euler differences over subsequent data records, and synchrophasor defined as $p(t) = a[n]\exp(j\varphi[n])$ with minimum latency in order to ensure compliance with standards requirements in terms of reporting rate.

3.1. Conventional Approaches

The most popular algorithms for PMUs are presented herein, with special focus on low computational complexity and good accuracy algorithms in various operating conditions.

3.1.1. Zero-Crossing and Root Mean Square

The zero-crossing technique is the approach proposed in the standard IEC 61000-4-30 for frequency estimation. It allows estimating the electrical signal frequency based on consecutive zero-crossing in the same direction (from positive to negative value or vice versa) of the electrical signal (currents or voltages). Let us note T_{zc} as the time between N_{zc} consecutive zero-crossings in the same direction. In this case, the frequency estimate is given by:

$$\widehat{f_g} = \frac{N_{zc}}{T_{zc}} \tag{2}$$

Unfortunately, this method is very sensitive to noise, harmonics, distorted signals, and many other PQ disturbances.

Root mean square (RMS) allows obtaining the amplitude of a signal based on the measurement of multiple of one half-cycle of the power system frequency. It is defined as the square root of the arithmetic mean of the squares of a set of signal samples and is mathematically given by:

$$X_{RMS} = \sqrt{\frac{1}{N}\sum_{k=1}^{N} x[k]^2} \tag{3}$$

This technique is very simple to implement but it is sensitive to noise and many PQ disturbances (spiking, flicker, etc.). Moreover, it does not provide an estimate of the phase angle parameter, which is mandatory to estimate the electrical phasor.

3.1.2. Taylor Weighted Least-Squares Algorithm

The Taylor Weighted Least-Squares (TWLS) algorithm is based on the Taylor Fourier transform (TFT) of a dynamic phasor model of an electrical waveform at nominal frequency. TWLS approximates the signal samples issued from PMUs using the Taylor series [110,111]. Indeed, in order to track phasor variations over time, phasor $p(t)$ defined at time distance $\Delta t = t - t_r$ from the reference time t_r can be approximated by its complex Taylor's series expansion around t_r as follows:

$$p(t) = p(t_r) + p^{'}(t_r)\Delta t + \frac{p^{''}(t_r)}{2!}\Delta^2 t + \ldots + \frac{p^K(t_r)}{K!}\Delta^K t, \quad |\Delta t| \leq \frac{T}{2} \tag{4}$$

where $p^k(t_r), k = 1, \ldots, K$ is the k^{th} order derivative of $p(t)$ computed at a reference time, which is assumed to be at the center of an acquisition duration T.

Based on signal acquisitions, coefficients of the Taylor series related to the r^{th} reference time can be estimated by the weighted least-squares (WLS) method [111]. WLS assumes the fundamental frequency to be equal to the nominal frequency. The theoretical background behind this approach can be found in [35,110]. Note that improvements of TWLS have been proposed, which allow dealing with the issue of off-nominal fundamental frequency [82]. Moreover, a real-valued TWLS has been proposed and demonstrated to be efficient for phasor estimation in [35]. TWLS is effective in dynamic conditions since it shows shorter synchrophasor and ROCOF estimate response times. However, this technique suffers from a poor ability to suppress harmonics, inter-harmonics, and wideband noise in a short data acquisition length.

3.1.3. Kalman Filtering

A Kalman filter is a recursive estimator that only requires the estimated state from the previous time step and the current measurement to compute the estimate for the current state. For synchronized phasor and frequency measurements, state variables are obtained from Taylor expansions of amplitudes and phase angles. Consequently, a dynamic model can be established, which allows estimating frequency and synchrophasors based on the Kalman filter theory, also known as linear quadratic estimation (LQE) [112].

Estimation of a synchronized phasor, frequency and ROCOF in time-varying conditions using Kalman filtering has been introduced in several works [37,113]. Harmonics are challenging when dealing with dynamic phasor estimation. Hence, many investigations have been conducted to include harmonics in the state space, and the Taylor–Kalman filter has been extended and enhanced to estimate both fundamental and harmonic phasors under dynamic conditions [112,114].

3.2. Power Spectral Density Estimation Techniques

Techniques presented herein can be classified into two main categories: the non-parametric techniques (precisely the periodogram and its extensions) and high resolution techniques.

3.2.1. Periodogram and Its Extensions

The power spectral density (PSD) $P_x(f)$ of a discrete-time signal is defined as the Fourier transform of its auto-correlation function [115]. The periodogram is a PSD estimate of a complex discrete-time wide sense stationary signal $x[n]$ and it is expressed as follows:

$$\widehat{P}_x(\omega) = \frac{1}{N}\left|\sum_{n=0}^{N-1} x[n]e^{\frac{-j\omega n}{F_s}}\right|^2 \tag{5}$$

where F_s is the sampling frequency and N is the number of samples.

The periodogram and its extensions are non-parametric methods, i.e., they do not require any a priori knowledge about the signal. The periodogram is often implemented using a Fast Fourier Transform (FFT) algorithm since it swiftly calculates the Discrete Time Fourier transform (DTFT) [116]. The DTFT phasor estimator is given by

$$\widehat{X} = \frac{1}{\sqrt{N}} \sum_{n=0}^{N-1} x[n] e^{\frac{-j\widehat{\omega_0} n}{F_s}} \tag{6}$$

where the angular frequency estimate $\widehat{\omega_o}$ is computed as follows:

$$\widehat{\omega_o} = \arg\max_{\omega} \widehat{P}_x(\omega) \tag{7}$$

Since the DTFT is computed for a finite length signal, the frequency resolution of the periodogram is low as it is equal to the inverse of the signal acquisition duration. Moreover, the accuracy of the periodogram is limited under frequency, amplitude, and phase variations. It should be noted that the periodogram is a biased (the distance between the single parameter being estimated and the average of the estimates is not equal to zero) and inconsistent estimator (when the data record length goes to infinity, the estimates variance does not decrease to zero) of the PSD [117]. This limitation can be overcome if several realizations $x_m[n]$ of the same random process $x[n]$ are available. This is performed using the Welch periodogram, which is defined as:

$$\widehat{P}_w(f) = \frac{1}{L} \sum_{k=1}^{k=L} \widehat{P}_{xw}^{(k)}(f) \tag{8}$$

where, $\widehat{P}_{xw}^{(k)}$ represents the periodogram of the windowed signal $x[n]w[n-\tau k]$, where $w[.]$ is a time window (Hanning, Hamming, etc.) and τ is a time delay.

The Welch periodogram allows increasing the estimation performance [118]. However, it decreases the spectral precision and resolution due to segmentation. Interpolated Discrete Fourier Transform (IpDFT) and its improvements, mainly the enhanced IpDFT [119] and the corrected IpDFT [120], are the most popular synchrophasor, frequency, and ROCOF estimation algorithms that use the DTFT for PMU measurements due to their low computational costs and the possibility to compensate for off-nominal frequency deviations [35,121].

3.2.2. High-Resolution Techniques

Parametric methods allow for higher resolutions than non-parametric methods in the case where the signal acquisition duration is short [122]. Indeed, if an a priori signal model can be assumed, parametric methods can be used to enhance the frequency resolution. These techniques are generally called high-resolution methods and include three categories: AutoRegressive Moving Average methods (ARMA), the subspace techniques, and the maximum likelihood estimation.

Subspace Techniques

Subspace methods for PSD estimation include: MUltiple SIgnal Characterization (MUSIC) and Estimation of Signal Parameters via Rotational Invariance Techniques (ESPRIT) approaches [122]. These approaches assume the noise to be a white Gaussian noise with zero mean and variance σ^2 and use Singular Value Decomposition (SVD) of covariance matrix of signal samples. Knowing the model order, it is possible to separate the signal and noise subspaces and consequently estimate the PSD.

MUSIC is based on the EigenValues Decomposition (EVD) of the covariance matrix $\mathbf{R}_{xx}$ of measurement data $\mathbf{x}[n] = [x[n], x[n+1], \ldots, x[n+M-1]]^T$ and the derivation of the associated eigenvectors. The MUSIC algorithm is provided by Algorithm 1.

Algorithm 1 MUSIC [123].

Require: N observations of the signal $\mathbf{x}[n]$.

1: Estimate the covariance matrix $\widehat{\mathbf{R}}_x = \frac{1}{G}\sum_{n=0}^{G-1}\mathbf{x}[n]\mathbf{x}[n]^H$. Where, N observations of $x[n]$ are used to construct $G = N - M + 1$ different subvectors, M is the length of the signal $\mathbf{x}[n]$ and $(.)^H$ refers to Hermitian matrix transpose.

2: Perform the eigenvalues decomposition of the covariance matrix $\widehat{\mathbf{R}}_x$ as follows

$$\widehat{\mathbf{R}}_x = \mathbf{V}\mathbf{\Sigma}\mathbf{V}^H \tag{9}$$

where, $\mathbf{V}$ is composed of the M orthonormal eigenvectors of $\widehat{\mathbf{R}}_x$, and $\mathbf{\Sigma}$ is a diagonal matrix of the corresponding eigenvalues σ_k sorted in decreasing order.

3: Estimate the model order L using model order selection techniques [124].

4: Compute the cost function

$$\mathcal{J}(f) = \frac{1}{\left\|\mathbf{v}^H(f)\widehat{\mathbf{N}}\right\|_F^2} \tag{10}$$

where, $\|.\|_F$ denotes the Frobenius norm and the column vector $\mathbf{v}(f)$ is given by

$$\mathbf{v}(f)^H = [1, e^{\frac{j2\pi f}{F_s}}, e^{\frac{2j2\pi f}{F_s}}, \ldots, e^{\frac{(M-1)j2\pi f}{F_s}}] \tag{11}$$

$\widehat{\mathbf{N}}$ is composed of the $M - L$ less significant eigenvalues σ_k spanning the noise subspace [125].

5: Frequency estimates $\widehat{f_k}$ correspond to the L largest peaks of $\mathcal{J}(f)$.

6: **return** Frequency estimates $\widehat{f_k}$ with $1 \leq k \leq L$.

MUSIC gives the pseudo-spectrum. Indeed, unlike the periodogram, MUSIC computes the signal frequency content without providing their amplitudes [126]. To overcome this issue, RootMUSIC has been investigated. It allows estimating the discrete frequency spectrum, along with the corresponding signal power estimates. Unfortunately, the computational burden of MUSIC is higher compared with classical approaches. Moreover, its performance depends on the covariance matrix estimate and the signal to noise ratio (SNR). To reduce the computational cost of MUSIC, the ESPRIT algorithm has been presented. Indeed, this technique is based on matrix eigenvalues calculation, which allows directly computing the signal spectrum, rather than leading to an optimization problem, which is the case for MUSIC [127]. The ESPRIT method is given by Algorithm 2. Since the ESPRIT approach gives only the frequency content, least square estimation is usually used for the frequency bin's amplitude estimation [115].

These approaches are more appropriate for discrete spectra and provide high-resolution frequency estimates. However, both techniques require the knowledge of the number of the frequency components, and their performances degrade under low SNR.

Algorithm 2 ESPRIT [123].

Require: N observations the signal $\mathbf{x}[n]$.

1: Estimate the covariance matrix $\widehat{\mathbf{R}}_x = \frac{1}{G}\sum_{n=0}^{G-1}\mathbf{x}[n]\mathbf{x}[n]^H$. Where N observations of $x[n]$ are used to construct $G = N - M + 1$ different subvectors, M is the length of the signal $\mathbf{x}[n]$ and $(.)^H$ refers to Hermitian matrix transpose.

2: Perform the eigenvalues decomposition of the covariance matrix $\widehat{\mathbf{R}}_x$ as follows

$$\widehat{\mathbf{R}}_x = \mathbf{V}\mathbf{\Sigma}\mathbf{V}^H \tag{12}$$

where $\mathbf{V}$ is composed of the M orthonormal eigenvectors of $\widehat{\mathbf{R}}_x$, and $\mathbf{\Sigma}$ is a diagonal matrix of the corresponding eigenvalues σ_k sorted in decreasing order.

3: Estimate the model order L using model order selection approaches [124].

4: Estimate the signal subspace $\widehat{S}_v$ composed of eigenvectors corresponding to the L largest eigenvalues.

$$\begin{aligned}\widehat{S}_{v1} &= [I_{M-1}\ \ 0]\widehat{S}_v \\ \widehat{S}_{v2} &= [0\ \ I_{M-1}]\widehat{S}_v\end{aligned} \tag{13}$$

5: Perform the eigendecomposition of $\widehat{S}_{v12} = [\widehat{S}_{v1}\ \ \widehat{S}_{v2}]$

$$\widehat{S}_{v12} = \boldsymbol{P}\Lambda\boldsymbol{P}^H \tag{14}$$

and partition $\boldsymbol{P}$ into $L \times L$ submatrices as follows

$$\boldsymbol{P} = \begin{bmatrix}\boldsymbol{P_{11}} & \boldsymbol{P_{12}} \\ \boldsymbol{P_{21}} & \boldsymbol{P_{22}}\end{bmatrix} \tag{15}$$

6: Compute Ψ_k the eigenvalues of $\Phi = -\boldsymbol{P_{12}}\boldsymbol{P_{22}}^{-1}$

7: Frequency estimates are given by

$$\widehat{f_k} = \frac{\angle(\Psi_k)}{2\pi} \tag{16}$$

where, $\angle(.)$ corresponds to phase angle.

8: **return** Frequency estimates $\widehat{f_k}$ with $1 \leq k \leq L$.

Maximum Likelihood Estimation

Statistical performance of the previously presented frequency estimation methods are inherently suboptimal and critically degrade under off-nominal conditions. To overcome this issue, the maximum likelihood estimation has been proposed. Indeed, the MLE has the distinct advantage of being asymptotically optimal for large enough data records [128]. Under white Gaussian noise assumption, the MLE for the fundamental frequency and the complex phasor is given by [129,130]

$$\{\widehat{\omega_0}, \widehat{\mathbf{S}}\} = \arg\max_{\omega_0, \mathbf{S}} \|\mathbf{X} - \mathbf{G}(\omega)\mathbf{S}\|_F^2 \tag{17}$$

where:

- $\mathbf{X}$ is a $N \times 3$ matrix containing the measured three-phase samples and is given by

$$\mathbf{X} = \begin{bmatrix} x_1[0] & x_2[0] & x_3[0] \\ \vdots & \vdots & \vdots \\ x_1[N-1] & x_2[N-1] & x_3[N-1] \end{bmatrix} \tag{18}$$

- $\mathbf{G}(\omega)$ is a $N \times 2$ real-valued matrix and is given by

$$\mathbf{G}(\omega) = \begin{bmatrix} 1 & 0 \\ \vdots & \vdots \\ \cos[(N-1)\omega_0] & \sin[(N-1)\omega_0] \end{bmatrix} \tag{19}$$

- $\mathbf{S}$ is a 2×3 real-valued matrix given by

$$\mathbf{S} = \begin{bmatrix} a_1 \cos(\Phi_1) & a_2 \cos(\Phi_2) & a_3 \cos(\Phi_3) \\ -a_1 \sin(\Phi_1) & -a_2 \sin(\Phi_2) & -a_3 \sin(\Phi_3)] \end{bmatrix} \tag{20}$$

- $\|.\|_F^2$ is the Frobenius norm.

It is worth noticing that this optimization problem can be divided into two steps, which are: (1) estimation of ω_0 by maximizing a one-dimensional function that can be easily optimized based on the Newton–Raphson algorithm, for instance [129], and (2) estimation of $\mathbf{S}$, which is computed by replacing ω_0 with its estimate $\widehat{\omega_0}$. This approach allows taking the benefits of the multi-dimensional nature of electrical signals. Moreover, it gives a high performance under noisy environments, harmonics, interharmonics, and off-nominal operating conditions, which meet the requirement of the IEEE std. C37.118.2011 standard [129].

3.3. Demodulation Techniques

Demodulation techniques rely on the estimation of the analytic signal $z[n]$ of a real-valued signal $x[n]$. These techniques can be classified into two categories: mono-dimensional and multi-dimensional techniques [131].

Let us denote $x[n] = a[n]\cos[\Phi[n]]$ a real-valued signal corresponding to a single-phase electrical signal (voltage or current). The corresponding analytic signal is given by

$$z[n] = a[n]e^{j\Phi[n]} \tag{21}$$

Based on the analytic signal, the instantaneous amplitude (IAm) $a[n] > 0$ and the instantaneous frequency (IF) $f[n] > 0$ can be simply be estimated as

$$\widehat{a}[n] = |z[n]| \tag{22a}$$

$$\widehat{f}[n] = \frac{1}{2\pi}(\angle(z[n+1]) - \angle(z[n])) \times F_s \tag{22b}$$

where F_s is the sampling rate and $|.|$ and $\angle(.)$ are the modulus and argument of a complex-valued signal $z[n]$, respectively.

3.3.1. Mono-Dimensional Techniques

The mono-dimensional techniques require a 1-D signal in order to compute the IA and IF.

Synchronous Demodulator

To detect the modulation introduced by PQ disturbances in power systems, a synchronous demodulation can be performed to estimate IA and ROCOF. A synchronous demodulator is also known as a Frequency Down-Conversion and Low-Pass Filtering (DCF) technique [38], which is described in the IEEE/IEC Standard $60255-118-1:2018$. Let us consider that the instantaneous phase is given by: $\Phi[n] = 2\pi f_0 n + \varphi[n]$ and assume that the fundamental frequency f_0 is known, which is usually the case for power grid signals (50 or 60 Hz) [122]. The synchronous demodulation is based on multiplying the signal $x[n]$ by two conjugate reference signals $\cos(2\pi f_0 n/F_s)$ and $\sin(2\pi f_0 n/F_s)$. Low-pass filtering of the output gives two low-frequency signals that correspond to IA and IF. A Butterworth low-pass filter with cut-off frequency around the nominal frequency can be

used to compute the direct or quadrature components. The SD scheme is illustrated in Figure 6 [132].

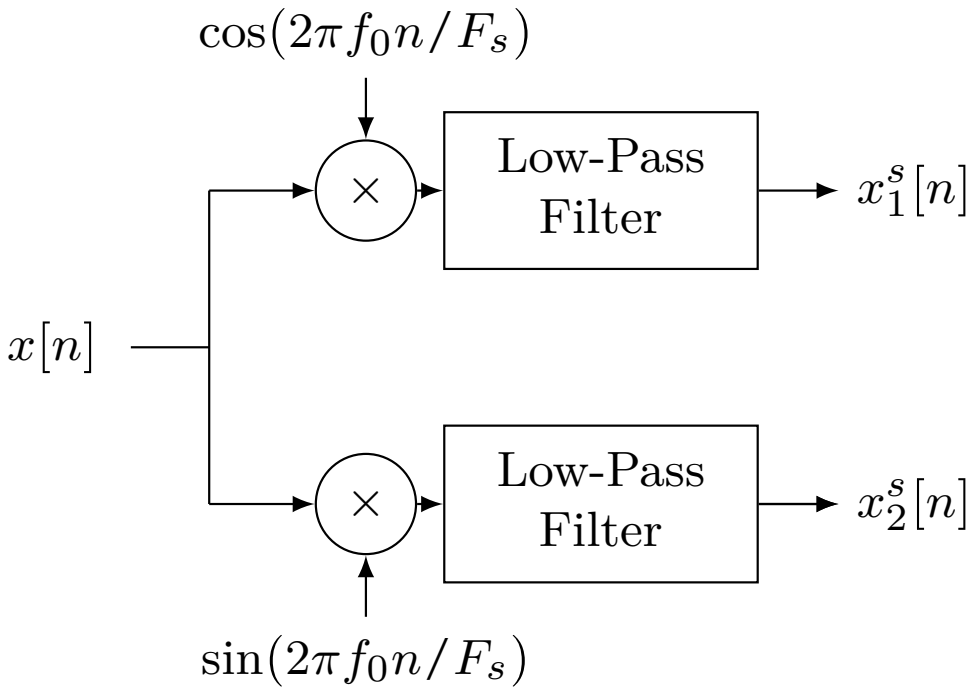

Figure 6. Synchronous demodulator.

The discrete time analytic signal can be computed as follows

$$z^s[n] = x_1^s[n] + jx_2^s[n] = a[n]e^{j\varphi[n]} \tag{23}$$

One of the drawbacks of the SD, i.e., DCF, approach is the filtering stage tuning and a slow convergence [133]. Moreover, IA and ROCOF estimation performance depends upon the chosen low-pass filter and assumes preliminary fundamental frequency measurement, mainly using IpDFT.

Hilbert Transform

Hilbert transform (HT) is a widely used technique in the signal processing community for the computation of the analytic signal. The Hilbert transform for a discrete signal $x[n]$ is given by [134]

$$x^h[n] = \sum_{-\infty}^{\infty} h[n-m]x[n], \tag{24}$$

where $h[n]$ is an impulse response, which is defined as

$$h[n] = \begin{cases} \frac{2}{\pi}\frac{\sin^2(\frac{\pi n}{2})}{n}, & n \neq 0, \\ 0, & n = 0. \end{cases} \tag{25}$$

Figure 7 shows how a discrete-time Hilbert transformer system can be used to form a complex analytic signal, which is simply a pair of real signals [135].

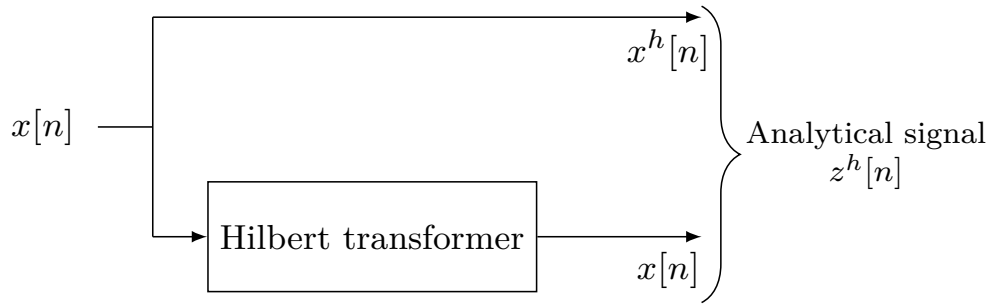

Figure 7. Block diagram representation of the Hilbert transform.

The Bedrosian theorem states that the uniqueness of the IF and the IA is satisfied if and only if the spectra of the IA and the sinus of the instantaneous phase are disjoint as depicted by Figure 8 [136]. Assuming Bedrosian conditions are satisfied, the analytic signal $z^h[n]$ associated with the real valued signal $x[n]$ is defined as [137].

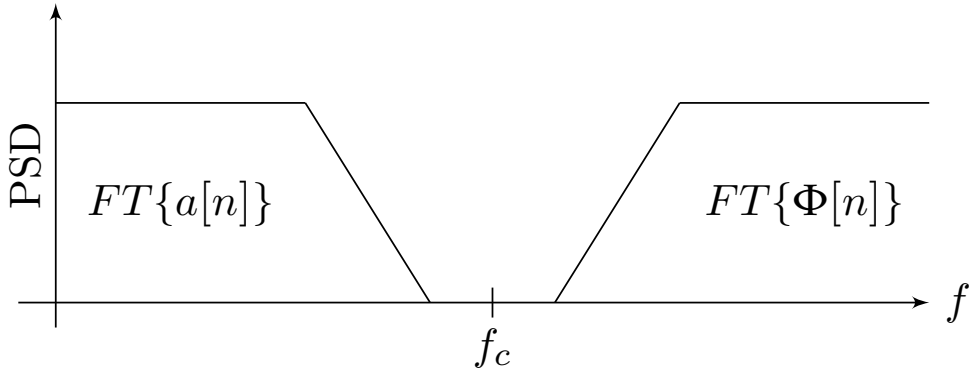

Figure 8. Illustration of the Bedrosian theorem conditions.

$$z^h[n] = x[n] + jx^h[n] = a[n]e^{j\Phi[n]} \tag{26}$$

It is worth mentioning that the Hilbert transform can be efficiently calculated for a real valued N-observations discrete time signal using the FFT algorithm [138]. One of the drawbacks of HT is the border effect [73].

Teager Energy Operator

The discrete-time Teager energy operator (TEO) is given by [139]

$$\Psi(x[n]) = x^2[n] - x[n+1]x[n-1] \tag{27}$$

TEO allows computing the IF and IA of a modulated signal without computing the analytic signal [140]. From the previous equation, it can be seen that the TEO is a local operator, which allows capturing the energy fluctuations with good time resolution since it requires only three samples ($x[n-1]$, $x[n]$, and $x[n+1]$). The Energy Separation Algorithm (ESA) allows estimating the IA and IF of a signal based on the TEO and is given by:

$$a[n] \approx \sqrt{\frac{\Psi[x[n]]}{1 - \left(1 - \frac{\Psi[x[n] - x[n-1]]}{2\Psi[x[n]]}\right)^2}} \tag{28a}$$

$$f[n] \approx \frac{1}{2\pi} \arccos\left(1 - \frac{\Psi[x[n] - x[n-1]]}{2\Psi[x[n]]}\right) \tag{28b}$$

The ESA offers interesting properties since it has less computational burden and has better time resolution than other demodulation techniques. The main disadvantage of this

operator is its sensitivity to noise and model mismatch. Moreover, it assumes that the estimated IF does not vary too fast or too greatly compared to the nominal frequency [141,142].

3.3.2. Multi-Dimensional Techniques

The multi-dimensional techniques exploit the three-dimensional nature of electrical signals in power systems.

Let us denote: $\mathbf{x}[n] = [x_1[n], x_2[n](t), x_3[n]]^T$ the 3×1 vector composed of the three phase electric signals measurements, which can be expressed as follows:

$$\begin{cases} x_1[n] = d_1 \times a[n] \cos[\Phi[n]] \\ x_2[n] = d_2 \times a[n] \cos[\Phi[n] - \frac{2\pi}{3}] \\ x_3[n] = d_3 \times a[n] \cos[\Phi[n] - \frac{4\pi}{3}] \end{cases} \tag{29}$$

where d_1, d_2 and d_3 correspond to the phase unbalance parameters.

Concordia Transform

Concordia transform (CT) is a multi-dimensional linear transform, which allows extracting two orthogonal components from three-phase voltages or currents assuming a balanced three-phase system. Let us denote $\mathbf{x}^c[n] = \left[x_1^c[n], x_2^c[n]\right]^T$ the two Concordia components, CT can be expressed as follows:

$$\mathbf{x}^c[n] = \begin{bmatrix} x_1^c[n] \\ x_2^c[n] \end{bmatrix} = \sqrt{\frac{2}{3}} \begin{bmatrix} \frac{\sqrt{2}}{\sqrt{3}} & -\frac{1}{\sqrt{6}} & -\frac{1}{\sqrt{6}} \\ 0 & \frac{1}{\sqrt{2}} & -\frac{1}{\sqrt{2}} \end{bmatrix} \mathbf{x}[n] \tag{30}$$

Under the assumption of a balanced three-phase system, the analytic signal $z^c[n]$ is given by [143]

$$z^c[n] = x_1^c[n] + j x_2^c[n] = a[n] e^{j\Phi[n]} \tag{31}$$

The main drawback of CT relies on the assumption of a balanced power system, which makes it unsuitable for most PQ disturbance analyses. Indeed, this assumption is not applicable for three-phase power systems under abnormal operating conditions [144].

Principal Component Analysis

Principal Component Analysis (PCA) is a statistical approach for reducing the dimensionality of dataset. Indeed, PCA transforms a number of correlated signals into a small number of uncorrelated components, called the principal components and denoted $\mathbf{x}^p[n] = \left[x_1^p[n], x_2^p[n]\right]^T$. PCA of a discrete signal $\mathbf{x}[n]$ can be mathematically expressed as follows:

$$\mathbf{x}^p[n] = \begin{bmatrix} x_1^p[n] \\ x_2^p[n] \end{bmatrix} = \beta \Lambda^{\frac{-1}{2}} \mathbf{S}^T \mathbf{x}[n] \tag{32}$$

where β is a scaling term given by

$$\beta = \sqrt{\frac{Tr[\mathbf{R}_x]}{3}} \tag{33}$$

where, Tr[.] corresponds to the sum of elements of the main diagonal. The covariance matrix $\mathbf{R}_x$ of $\mathbf{x}[n]$ can be expressed as follows:

$$\mathbf{R}_x = E[\mathbf{x}[n]\mathbf{x}^T[n]] = \mathbf{U}\Lambda\mathbf{U}^T \tag{34}$$

with, Λ and $\mathbf{U} = [\mathbf{S}\ \mathbf{G}]$ are matrices composed of the eigenvalues and eigenvectors of $\mathbf{R}_x$, respectively.

Under the assumptions that $\Phi[n]$ is uniformly distributed in $[0; 2\pi]$ and that $a[n]$ and $\Phi[n]$ are statistically independent, the analytic signal $z^p[n]$ can be estimated up to a phase indetermination as follows:

$$z^p[n] = x_1^p[n] + jx_2^p[n] = a[n]e^{j\Phi[n]}e^{-j\theta}. \quad (35)$$

where, θ is an unknown phase.

As opposed to the Concordia transform, PCA is applicable for three-phase systems analysis regardless of the balance assumption [145]. Consequently, PCA is less restrictive and is interesting for unbalanced power systems analysis and PQ disturbances detection.

3.4. Time-Frequency, Time-Scale Analysis

Spectral estimation techniques are badly suited for PQ monitoring under nonstationary environments due to transient or faulty operating conditions. In nonstationary conditions, disturbance detection is usually performed based on time-frequency and time-scale representations. These approaches include and are not limited to: Short-Time Fourier Transform (STFT), Continuous Wavelet Transform (CWT), Wigner–Ville Distribution (WVD) and other quadratic distributions, and the Hilbert–Huang Transform (HHT). For more details regarding time-frequency representations, readers can refer to [146–148].

3.4.1. Spectrogram

The spectrogram is based on the computation of the Short Time Fourier Transform (STFT), $S_x[m, l]$, of a signal $x[n]$ and is defined as the squared absolute value of the STFT, i.e., $|S_x[m, l]|^2$. It assumes the electrical signals to be quasi-stationary over a short time duration and is derived by computing the Fourier transform of consecutive time-frames, which may be overlapping. STFT is performed based on three stages as follows:

- The electric signal $x_k[n]$ is divided into time segments,
- A time window $h[.]$ is applied to each segment to reduce side-lobe effects. Classical choices for $h[n]$ is the rectangular, Hanning, Hamming or Gaussian windows.
- PSD estimation of each windowed time segment is calculated based on the Fourier transform.

STFT leads to a 3-D representation, which allows determining the sinusoidal frequency and phase content of local sections of an electric signal as it changes over time. Let us consider discrete signals of period N and a time window $h[n]$ (symmetric discrete signal of period N) with norm $\|h\| = 1$. The discrete STFT is mathematically expressed as follows [149]:

$$S_x[m, l] = \sum_{n=0}^{N-1} x[n]h[n - m] \exp\left(\frac{-j2\pi ln}{N}\right) \quad (36)$$

For each $0 \leq m \leq N$, $S_x[m, l]$ is calculated for $0 \leq l \leq N$ with N fast Fourier transform (FFT) procedures of size N. The STFT is a linear, transform i.e., $S_{x+y}[m, l] = S_x[m, l] + S_y[m, l]$. The length of the window $h[n]$ determines the time and frequency resolution of the time–frequency representation. STFT is a mono-resolution approach (Figure 9a), i.e., the resolution remains the same in the time–frequency plane. In fact, a short time window leads to a representation, which is fine in time but coarse in the frequency domain. Contrariwise, a long window leads to a representation, which is coarse in time but fine in the frequency domain regardless of the frequency range [150]. This trade-off is known as the Heisenberg–Gabor uncertainty space [146].

3.4.2. Scalogram

The Scalogram is based on the computation of the Discrete Wavelet Transform (DWT). DWT is performed by breaking up the signal into shifted and scaled versions of a mother

wavelet (Haar, Daubechies, Mexican Hat, etc.) and is mathematically expressed as follows [149]:

$$T_x[n, a^l] = \sum_{m=0}^{N-1} x[m]\xi_l^*[m-n] \tag{37}$$

where $(.)^*$ denotes the complex conjugate, a^l is the scale, and $\xi_l[n]$ is the mother wavelet. A discrete wavelet scaled by a^l is defined by

$$\xi_l[n] = \frac{1}{\sqrt{a^l}}\xi\left(\frac{n}{a^l}\right) \tag{38}$$

The DWT is a linear transform, i.e., $T_{x+y}[n, a^l] = T_x[n, a^l] + T_y[n, a^l]$. DWT leads to a time-scale representation as it gives the signal time-evolution at different scales. However, there is a direct link between the scale and frequency. Indeed, if the central frequency of the mother wavelet $\xi(t)$ is f_0, the scale a^l focuses on the frequency content at $f = f_0/a^l$. Unlike STFT, DWT is a multi-resolution technique, which provides high time resolution at high-frequencies and high frequency resolution at low frequencies (Figure 9b). Unfortunately, the wavelet transform is also limited by the Heisenberg–Gabor principle. Note that the scalogram is defined as the squared absolute value of the DWT, i.e., $\left|T_x[n, a^l]\right|^2$ [75,151].

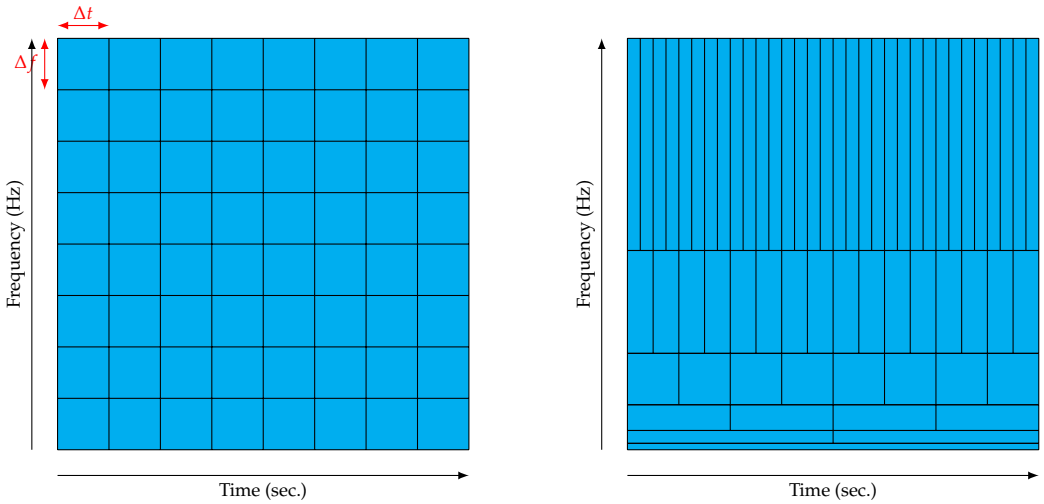

Figure 9. Time-frequency resolution. (**a**) Short Time Foutier Transform based mono-resolution approach. (**b**) Discrete Wavelet Transform-based multi-resolution approach.

3.4.3. Wigner–Ville and Other Quadratic Distributions

The STFT and DWT are linear transforms, which focus on the decomposition of the electrical signal samples. The Wigner–Ville distribution (WVD) allows the decomposition of the electrical signal energy in the time-frequency plane [152]. The WVD of a discrete signal $x[n]$ is defined by [149]:

$$W_{x,x}[n,k] = \sum_{p=-N}^{N-1} x\left[n+\frac{p}{2}\right]x^*\left[n-\frac{p}{2}\right]\exp\left(\frac{-j2\pi kp}{N}\right) \tag{39}$$

One of the major advantages of WVD is that the time–frequency resolution of the representation is not limited by the Heisenberg Gabor inequality. However, the WVD is a nonlinear transform, i.e., $W_{(x+y),(x+y)}[n,k] \neq W_{x,x}[n,k] + W_{y,y}[n,k]$, which introduces interference terms (artefacts) that may lead to misleading interpretations. In order to remove these cross-terms, a smoothed version of the Wigner–Ville distribution has been proposed. Moreover, the analytic signal is often used instead of the signal itself for interference terms

mitigation. Furthermore, several extensions of the WVD for interference reduction have been introduced at the expense of reduced resolution [152,153]. These extensions have been unified by the Cohen's class of time–frequency distributions [154]. The Cohen's class includes the Pseudo Wigner–Ville, the Choi–Williams, and the Zhao–Atlas–Marks Distributions [155].

3.4.4. Hilbert–Huang Transform

The Hilbert–Huang Transform (HHT) is well suited for nonstationary and nonlinear signals. It is the result of the Empirical Mode Decomposition (EMD) and the Hilbert spectral analysis (HSA) of signal measurements [85,156,157]. It is composed of three stages, as follows:

- The electrical signal is decomposed into a sum of amplitude- and frequency- modulated mono-component sine waves using an EMD algorithm. EMD has been proposed by Huang and is described by the following algorithm [158]:
  - Identification of all extrema of $x[n]$
  - Interpolation between minima (resp. maxima) ending up with some envelope $e_{min}[n]$ (resp. $e_{max}[n]$).
  - Computation of the mean:

$$m[n] = \frac{e_{min}[n] + e_{max}[n]}{2} \tag{40}$$

  - Extraction of the detail:

$$d[n] = x[n] - m[n] \tag{41}$$

  - Iteration on the residual $m[n]$.

In practice, this algorithm has to be refined by a *shifting process* until $d[n]$ can be considered as zero-mean. After this procedure, the detail $d[n]$ corresponds to an amplitude- and frequency-modulated (AM/FM) sine wave called Intrinsic Mode Function (IMF). By iterating the algorithm on the residual $m[n]$, the EMD extracts several IMFs until a stopping criterion is reached.

- Instantaneous amplitude and instantaneous frequency of each IMF are extracted using a demodulation technique described in Section 3.3. In general, to achieve IA and IF calculation, the Hilbert transform is used. In this case, the transformation is called HHT.
- The time-frequency representation is obtained by displaying the time evolution of the instantaneous amplitude and frequency for each sine wave in the time-frequency plane.

3.5. Discussion

The characterization of power system disturbances requires frequency and phasor estimation. This can be achieved based on PSD estimation techniques and time–frequency representation as previously discussed. PSD estimation techniques include two categories, which are the non-parametric and parametric approaches and are more adequate for steady state and stationary signals analysis. In the case of nonstationary signals, time–frequency is used to exhibit the varying behavior of the fundamental frequency, phasor, and harmonics. Figure 10 provides a classification of the PSD estimation methods and time–frequency analysis techniques for power quality monitoring [123].

Demodulation approaches for PQ monitoring present the advantage of being able to track the evolution of instantaneous amplitude and instantaneous frequency of the power system. These two parameters are of huge interest for PQ disturbances detection. Figure 11 provides an overview of the demodulation technique to use for PQ monitoring based on electrical signals analysis [131]. Especially, in the case of multi-component signals, a filtering step is required in order to separate modes. In the case where the modes cannot be separated using filtering, more sophisticated techniques are required such as Empirical

Mode Decomposition (EMD), Ensemble EMD (EEMD) [159,160] and Variational Mode Decomposition (VMD) [161,162].

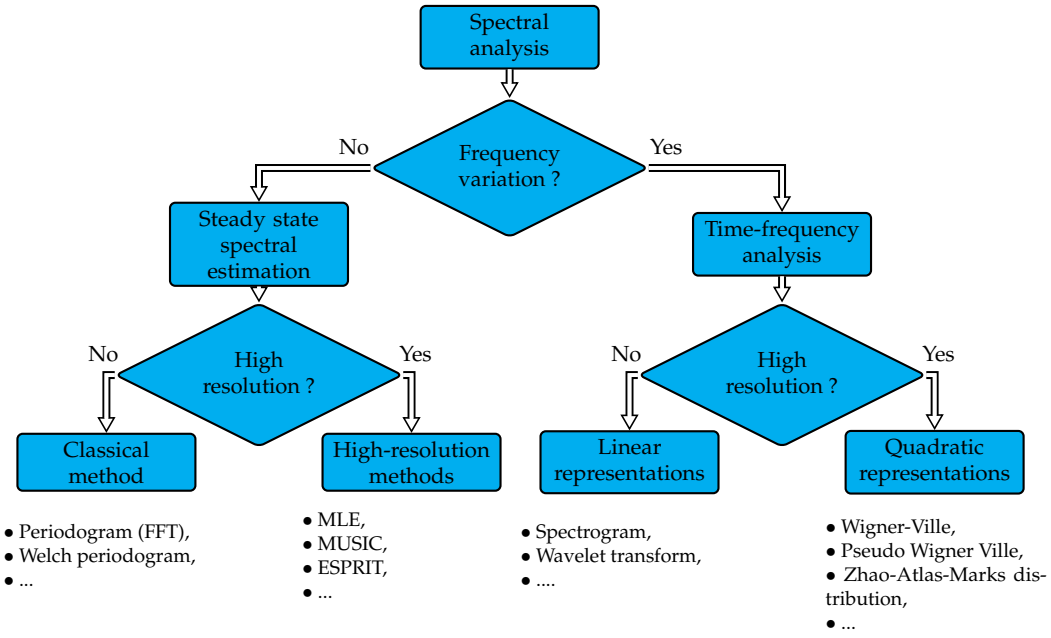

Figure 10. PQ features extraction based on power spectral density estimation and time-frequency representation.

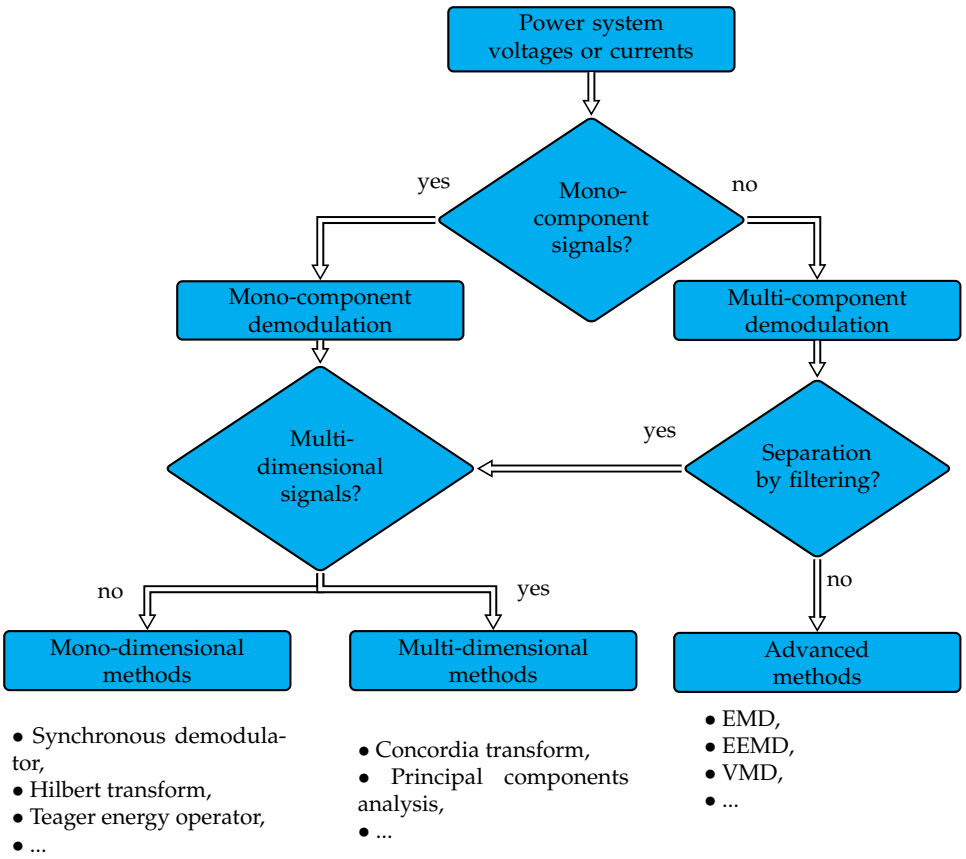

Figure 11. Demodulation techniques for PQ monitoring.

The Empirical Mode Decomposition (EMD) has been originally proposed by Huang [158] and Variational EMD (VMD) has been proposed by Dragomiretskiy and Zosso [163]. Both

EMD and VMD decompose a signal $x[n]$ into a small numer L of narrowband components as follows:

$$x[n] = \sum_{k=1}^{L} u_k[n] \tag{42}$$

where, $u_k[n] = a_k[n]\cos(\Phi_k[n])$ is an amplitude and frequency modulated signal, termed as Intrinsic Mode Function (IMF). Each IMF has a positive and slowly varying envelope an instantaneous frequency $f_k[n] = \frac{d\Phi_k[n]}{dt}$ that is nondecreasing, varies slowly, and is concentrated around a central value.

Using the EMD method, any nonstationary and nonlinear signal can be decomposed into a finite and often small number of components (IMFs). These IMFS form a complete and nearly orthogonal basis for the original signal. Unlike EMD, the variational mode decomposition technique simultaneously computes all the mode waveforms and their central frequencies [164,165]. The process consists of finding a set of $u_k[n]$ and $f_k[n]$ that minimizes the constrained variational problem [163]. EMD suffers from mode mixing, end effects, and best IMF selection and uniqueness. The mode mixing issue has been dealt with by introducing Ensemble EMD (EEMD) [166].

After IMFs computation and performing the demodulation based on the classical approaches (SD, HT, CT, PCA, etc.), the analytic signal and the corresponding IA and IF must be appropriately analyzed to assess the PQ disturbance. Several papers have proposed to monitor the deviation of the analytic signal from a circle in the complex plane [167]. This approach is appropriate for amplitude modulated electrical signals but is not convenient for frequency modulated signals as the disturbance only affects the rotational speed of the phasor in the complex plane. Hence, in order to perform a disturbance detection, the variance of the IA, $a[n]$ and the IF, $f[n]$ can be used for disturbance analysis.

4. Disturbances Classification Techniques

Disturbance characterization requires two steps, which are event detection by determining the starting and ending time of the event, and event classification. Power quality disturbance classification is of paramount importance as it allows identifying and classifying power system abnormal operating conditions. Several approaches have been investigated in the literature for power quality monitoring and behavior analysis. These techniques can be classified into two classes: Conventional approaches and machine learning approaches.

4.1. Conventional Approaches for Quality Monitoring

Power quality disturbances such as voltage sags and swells are generally characterized based on the amplitude and duration. Almost all classical approaches do not require phasor (phase angle) and other parameters for fault characterization. In this subsection, three classical approaches are briefly discussed, which are ABC classifier, symmetrical component classifier and model order selection method.

4.1.1. ABC Classifier

ABC classification is used to characterize voltage sag types [99,168]. It was developed to analyze the propagation of a voltage sag from transmission to distribution networks when a disturbance propagates through a transformer. Voltage sags classification is derived based on the combination of the three following factors [83]:

- Fault type, which includes single-line-to-ground fault, line-to-line fault, double-line-to-ground fault, three-phase fault,
- Transformer winding connection,
- Load connection.

There are seven basic voltage sag types according to the ABC classification, as depicted by Figure 12.

4.1.2. Symmetrical Component Classifier

Symmetrical component classification is more general than the ABC classifier. It gives a direct relationship with measured voltages but is harder to understand. Consequently, a translation to the ABC classification may be more adequate for many applications. It mainly allows classifying the six possible sub-types of voltage sag of type C and type D [84]. Symmetrical components have been introduced by Fortescue in order to analyze three-phase systems under both normal and abnormal (disturbances presence) operating conditions. This transform allows obtaining a sparse mathematical representation of the three-phase system, namely the space vector and homopolar component. To define these two quantities, let us consider the following three-phase signals (voltages or currents) model:

$$x_k[n] = \sum_{h=1}^{H} a_{kh} \cos(h \times \omega_0 n + \phi_{kh}) + b_k[n] \tag{43}$$

where ω_0 is the angular fundamental frequency, a_{kh} and ϕ_{kh} are the amplitude and the initial phase of the k^{th} phase ($k = 0, 1, 2$) and h^{th} harmonic ($h = 1, 2, \ldots, H$), and $b_k[n]$ is the additive noise.

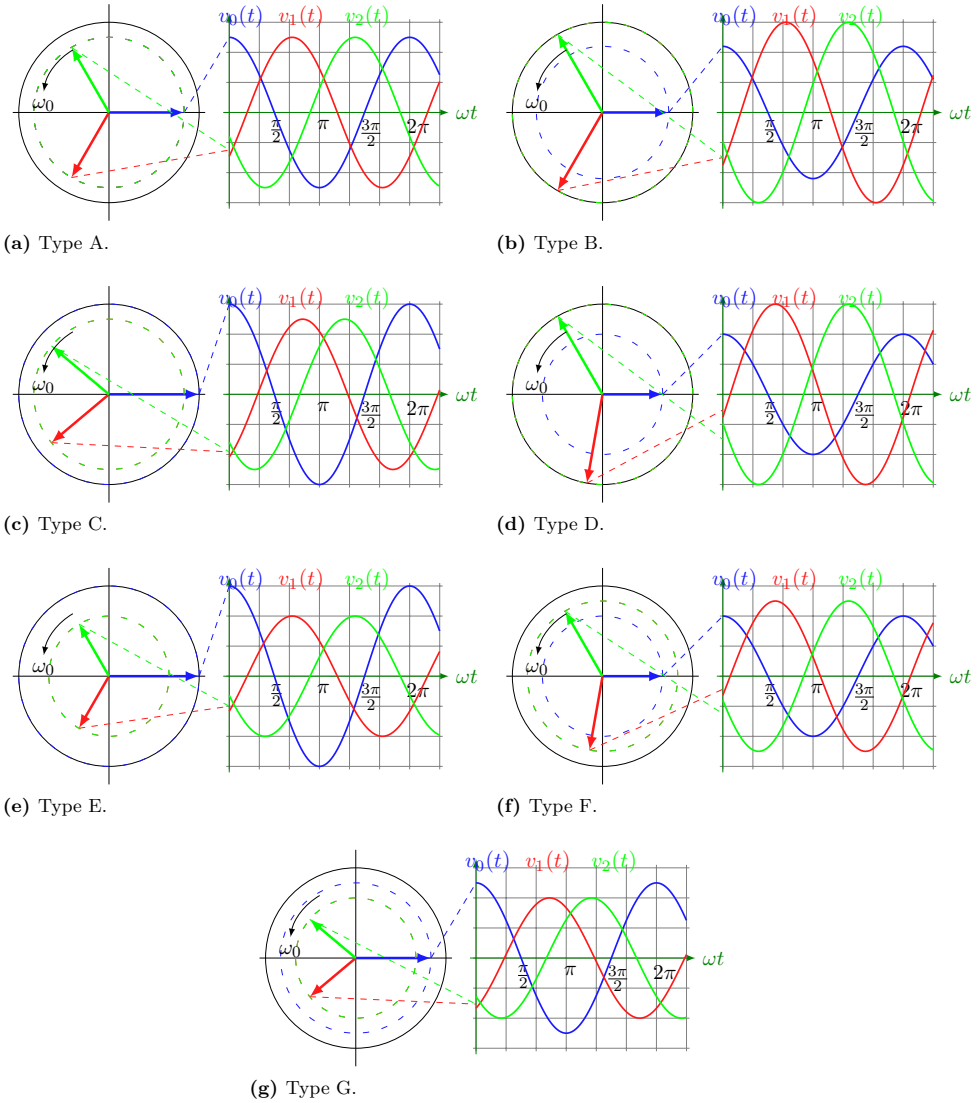

(a) Type A. **(b)** Type B.

(c) Type C. **(d)** Type D.

(e) Type E. **(f)** Type F.

(g) Type G.

Figure 12. Voltage sag types according to [99] (solid line circle corresponds to the nominal amplitude before fault).

Applying the Fortescue transform (symmetrical components analysis) allows obtaining the following electrical quantities of interest:

$$\begin{bmatrix} \underline{x}[n] \\ x_z[n] \end{bmatrix} = \frac{2}{3} \begin{bmatrix} 1 & e^{j\frac{2\pi}{3}} & e^{j\frac{4\pi}{3}} \\ \frac{1}{2} & \frac{1}{2} & \frac{1}{2} \end{bmatrix} \begin{bmatrix} x_0[n] \\ x_1[n] \\ x_2[n] \end{bmatrix} \tag{44}$$

where, $\underline{x}[n]$ is termed the space vector and $x_z[n]$ corresponds to the hompolar component (zero-sequence), which is null for balanced and non-connected neutral point three-phase systems.

Fundamental Frequency Deviation

In Europe, the power grid fundamental frequency value is equal to 50 Hz, with acceptable frequency deviation equal to ± 1 Hz [16,169]. Power grid frequency variations are totally unpredictable and are mainly due to the mismatch between electricity production and consumption. Indeed, electricity storage, in any significant quantity, is very limited so it must be consumed at the instant it is generated. Measurement and evaluation of fundamental frequency deviation from its nominal value can be assessed through the ROCOF, which is defined as follows:

$$ROCOF = \frac{1}{2\pi} \frac{d\omega_0}{dt} \tag{45}$$

Fundamental Amplitude and Phase Shift Related Disturbances

A power grid is a three-phase system that has a mutual coupling between phases. A balanced three-phase system is composed of three sinusoidal waveforms characterized by the same fundamental frequency that is equal to the nominal value, amplitudes equal to 1 pu, and phase shift between phases equal to $\pm 120^\circ$. If one of these conditions is not satisfied, the system is considered as unbalanced. Unbalance is generally due to asymmetrical loads: active loads cause amplitude deviations and reactive loads cause phase shifts to vary from the normal value of $\pm 120^\circ$. The unbalance is estimated based on the computation of symmetrical components as follows:

$$U_f = \left| \frac{x_0[n] + x_1[n]e^{j\frac{4\pi}{3}} + x_2[n]e^{j\frac{2\pi}{3}}}{x_0[n] + x_1[n]e^{j\frac{2\pi}{3}} + x_2[n]e^{j\frac{4\pi}{3}}} \right| \times 100 \tag{46}$$

Voltage sags are the most frequent disturbances in a power grid and therefore the most troublesome for the industry. Indeed, this disturbance can lead to production losses and even degradation of product quality. In most cases, voltage sags are caused by short circuits. Depending on the type and location of the short-circuit, as well as the transformer's neutral regime and the measurement method (between phases or between phases and ground), different types of voltage dips can be distinguished (signatures). Specifically, a distinction can be made between the single-phase, two-phase and three-phase voltage dips. The single and two-phase voltage sags are also called unbalanced. The unbalance depends on phase angle shifts and amplitudes of the phases affected by the voltage dip.

Overvoltages (voltage swell) and overcurrents can also affect the power quality in a power grid. Overvoltages are caused by large load triggering, voltage regulator abnormal operation, resonance and maneuvers. Overcurrents are mainly due to short-circuits and can lead to voltage sag. In some circumstances, voltage sags and swells can appear at the same time. In this case, they are characterized by voltage drops on one or two phases and overvoltages on the other phases. This power quality disturbance type is mainly caused by short-circuits affecting three-phase systems with non-connected neutral point or high impedance earthed systems. In this case, only the homopolar component is affected by the fault due to abnormal displacement voltage of a neutral point.

Considering the particular case where only the fundamental frequency component exists, three-phase systems are composed of sinusoidal waveforms ($H = 1$) at the same fundamental frequency. In this case, the space vector is expressed as follows:

$$\underline{x}[n] = x_p[n]e^{j\omega_0 n} + x_n[n]e^{-j\omega_0 n} \tag{47}$$

where, $x_p[n] = |x_p[n]|e^{j\phi_p}$ and $x_n[n] = |x_n[n]|e^{j\phi_n}$ are phasors rotating in the complex plane counterclockwise and clockwise directions, respectively.

In the case where one of the two phasors is null, the space vector describes a circle in the complex plane. In this case, if the homopolar component is zero, the three-phase system is considered as balanced and corresponds to the normal operating conditions. However, in case of fundamental frequency related disturbances, the space vector takes the form of an ellipse in the complex plane with parameters as follows

$$\begin{cases} r_{max} = x_p[n] + x_n[n] \\ r_{min} = x_p[n] - x_n[n] \\ \phi_{tilt} = \frac{1}{2}(\phi_p + \phi_n) \end{cases} \tag{48}$$

Harmonics Disturbances

Harmonic disturbances are due to the integration into the power grid of nonlinear loads such as power electronics equipment (motor drives, inverters, static converters, etc.). Harmonics cause heating, which increases power system losses and reduces the life span of the equipment. They can also cause equipment malfunctioning (synchronization, switching) and measurements errors. In the case of harmonics disturbances, the space vector can be expressed as follows:

$$\underline{x}[n] = \sum_{h=1}^{H} \left[x_p[n]e^{jh\omega_0 n} + x_n[n]e^{-jh\omega_0 n} \right] \tag{49}$$

Harmonic disturbances can be analyzed based on the spectral analysis of the space vector and homopolar component. Harmonics can be localized in the space vector or homopolar component spectrum depending on the harmonics order. Indeed, when harmonics are distributed in a way that is uniform in all three phases, they form three-phase systems, namely, direct, inverse or homopolar depending on harmonics order. Thus, harmonics of rank $3 \times n + 1$ with $n \in \mathbb{N}$ form the direct system and appear only for positive frequencies in the space vector spectrum. Harmonics of rank $3 \times n - 1$ with $n \in \mathbb{N}$ form the inverse system and consequently appear only on the negative frequencies of the space vector spectrum. The harmonics of rank $3 \times n$ with $n \in \mathbb{N}$ form the homopolar system and therefore only appear in the homopolar component spectrum. In addition, the amplitude of the detected harmonics in the spectrum of the space vector or that of the homopolar component is equal to the amplitude of the harmonics in the original three-phase system. However, if harmonics are no longer evenly distributed over the three phases, they no longer purely form direct, inverse or homopolar systems. Consequently, harmonic components of the same rank appear both on the positive and negative frequency side of the space vector spectrum, as well as on the spectrum of the homopolar component. The analysis of the frequency content of the space vector and the homopolar component allows directly obtaining the average amplitude and the level of unbalance of each harmonic in the actual three-phase power system.

4.1.3. Information Criteria Rules

In [97], the authors proposed a novel approach for power quality disturbance classification based on the analysis of the three-phase signals. The focus is placed on voltage sags and swells, which are pre-classified into four classes that depend upon the non-zero symmetrical components under quasi-stationary conditions as follows:

- $\mathcal{C}_1$: Zero and negative sequences are null,
- $\mathcal{C}_2$: Zero sequence is null,
- $\mathcal{C}_3$: Negative sequence is null,
- $\mathcal{C}_4$: All sequences are not null.

This pre-classification stage is formulated as a model order selection problem and solved using information criteria rules [124]. The proposed approach has been evaluated for various signal acquisition durations, signal to noise ratios (SNR), quasi-stationary conditions and total harmonic distortion values. For more detail regarding the mathematical development, the readers are encouraged to refer to the following paper [97]. Note that the proposed classification is related to the commonly used ABC classification, as depicted by Table 3.

Table 3. Link between classes and ABC classification.

Type	Balanced or A	C, D, F and G	H and I	B and E
Proposed class	$\mathcal{C}_1$	$\mathcal{C}_2$	$\mathcal{C}_3$	$\mathcal{C}_4$

4.2. Machine Learning Techniques

Power quality monitoring systems allow continuous tracking of voltage and current in the transmission and distribution grid, and then intelligent systems analyze and interpret raw data with minimum human intervention. Moreover, Internet of Things (IoT) provides a platform for deploying a network of PQ monitoring devices for accurate and reliable data acquisition. Artificial intelligence (AI) techniques have been proposed and proven to be useful tools that allow providing real-time information for diagnostics and problem isolation, mainly during the decision process [170]. The AI techniques include several sophisticated approaches such as Fuzzy expert systems, artificial neural networks, support vector machines, and many others. These approaches have been widely investigated in power system monitoring for PQ disturbance classification, protection and consumption profile identification.

4.2.1. Artificial Neural Networks Technique

An artificial neural network (ANN) is the component of artificial intelligence that is meant to behave like interconnected human brain cells. Indeed, its design is schematically inspired by the operation of biological neurons of the human brain. The multilayer perceptron (MLP) is a class of feedforward artificial neural networks that is illustrated by Figure 13. An MLP is composed of at least three layers of nodes: an input layer, a hidden layer and an output layer. Each node of the hidden layers and output layer is a neuron that uses a nonlinear activation function. One neuron is the result of applying the nonlinear transformations of linear combinations of inputs x_i, weights w_i and biases b, as depicted by Figure 14. MLP is a supervised machine learning approach that uses a learning technique called backpropagation for training and allows distinguishing data that is not linearly separable by linear perceptron. Indeed, ANNs require a learning database composed of actual case examples that are used for the training stage [171]. The learning database must be sufficiently large depending on the structure and complexity of the problem under study. However, a large learning database can lead to an overfitting problem and thus degrading the neural networks performance (the neural network loses its ability to generalize). Indeed, there is a trade-off between generalization and over-training.

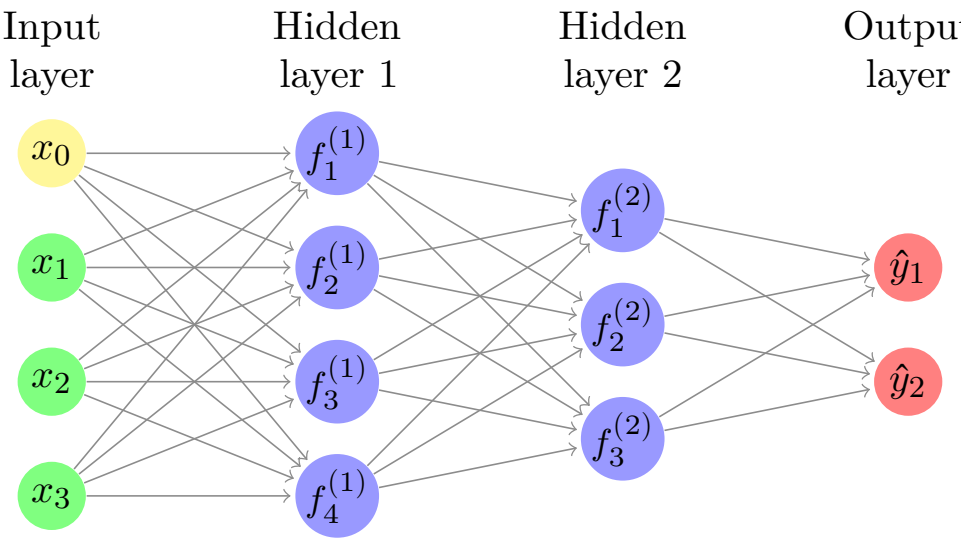

Figure 13. Multilayer perceptron (MLP) with 4 inputs, 2 hidden layers and 2 outputs.

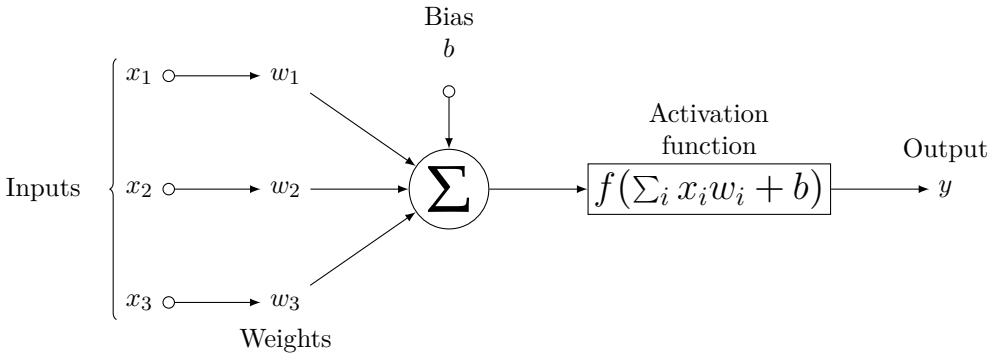

Figure 14. Illustration of basic neuron with n inputs.

PQ disturbance detection and classification, for both single and multiple disturbances under nonstationary and noisy environments, have been dealt with in several papers in the literature. Indeed, in [85,162,165], empirical mode decomposition and variational mode decomposition associated with Hilbert transform has been proposed for PQ features processing. Then, an online-sequential extreme learning machine is implemented to recognize the single as well as multiple power quality events. The proposed approach has been proven to have high anti-noise performance, less computational burden and high classification accuracy. Monedero et al. [88] and Valtierra-Rodriguez et al. [87] have investigated a challenging task related to the use of ANNs for real-time detection and classification of single and combined power quality disturbances.

4.2.2. Support Vector Machines Technique

In machine learning, support vector machines (SVM) are a set of supervised learning approaches with associated learning algorithms that are used for input data clustering, pattern recognition, and regression analysis [171]. For classification, let us suppose a given data point belonging to two separate classes. In support vector machine theory, each data point is considered as a p-dimensional vector and a $(p-1)$-dimensional hyperplane is used to separate such data points. Since there are many hyperplanes that allow classifying the data, the best choice is the one maximizing the distance from it to the nearest data point on each side (largest margin) as depicted by Figure 15. Similarly to ANNs, the SVM requires a training stage and actual labeled examples to set the model. SVM is based on statistical learning theory and consists of two steps. First, a nonlinear transform (ϕ) of input data to high dimensional space is performed. Then, an optimal hyperplane or set of

hyperplanes in a high- or infinite-dimensional space allowing to linearly classify the input data in this high-dimensional space is determined.

Many papers in the literature have proven that SVMs are well suited to deal with power system disturbances classification. In [172,173], the authors proposed the combination of a non-dominated sorting genetic algorithm for an effective features extraction from power signals and a directed acyclic graph support vector machine compared with several other machine learning techniques for disturbance classification. In [174], an adaptive chirp mode pursuit has been performed to extract useful features, and a grasshopper optimization algorithm is used to optimize the parameters of the SVM that are used for power quality disturbance classification. Moreover, in [175], the authors have compared SVM and MLP for voltage sag detection and classification under various PQ disturbance conditions for both synthetic and real data. Feature engineering stages have been performed using independent component analysis and high order statistics. Both approaches have showed good results for low acquisition duration (less than on half the cycle of the fundamental frequency). The support vector machine-based approach has been proposed in [176], which allow discriminating between islanding and grid fault events for a real-life practical photovoltaic plant.

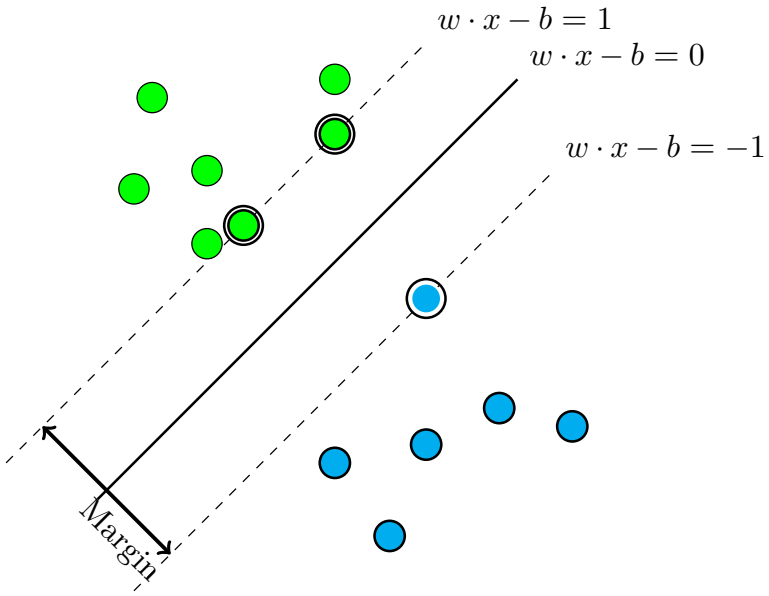

Figure 15. Maximum-margin hyperplane and margins for an SVM trained with samples from two classes.

4.2.3. Fuzzy Expert Systems

Unlike binary logic, fuzzy logic is a form of probabilistic logic, which is used to imitate human reasoning and cognition. Indeed, fuzzy logic variables may have truth values that ranges in degree from 0 to 1. Fuzzy logic is inspired by human reasoning to generalize the traditional combinatory logic under uncertainty. The greater generality of fuzzy logic is needed to deal with complex problems in the realms of search, question–answering decision and control. An illustration of a rule-based expert system architecture is provided in Figure 16. The fuzzy expert system uses fuzzy sets and fuzzy rules as a base rather than boolean sets. A fuzzy set is fully defined by the corresponding membership functions and fuzzy rules consist of human-like reasoning capabilities [177].

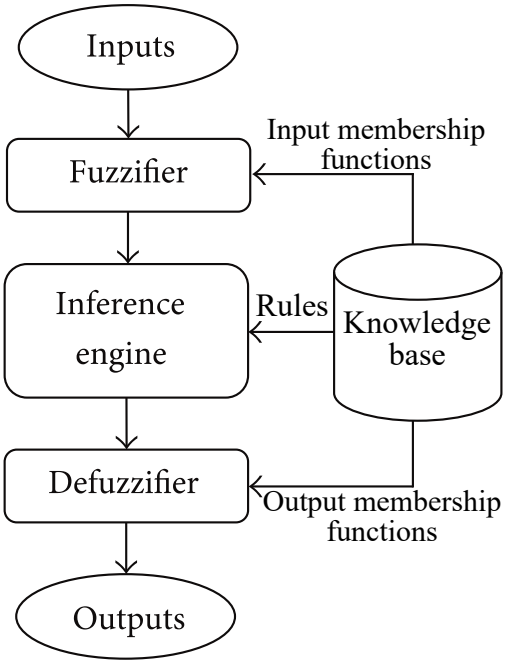

Figure 16. Block diagram of a fuzzy expert system.

The application of fuzzy expert systems for automatic power system fault detection and classification was carried out by various authors in previous studies [178–181]. Fuzzy expert systems for PQ monitoring purposes to classify events related to PQ disturbances via fuzzy if-then rules [182]. Adaptive fuzzy logic systems use the learning capabilities of ANNs or genetic algorithms to adjust model parameters and afterwards enhance the global PQ disturbances monitoring system performance [180,183,184].

4.2.4. Deep Learning Approaches

Deep learning (DL) is a class of machine learning algorithms that is based on artificial neural networks, specifically convolutional neural networks (CNN)s. CNNs consist of convolution layers followed by fully connected neural networks. DL uses multiple layers that allow to progressively extract higher level features from raw data. Indeed, signal analysis and the feature selection requires an expert and can be inaccurate, which leads to a low classification accuracy of multiple disturbances and a poor noise immunity. DL architectures include deep neural networks, deep belief networks, graph neural networks, recurrent neural networks and convolutional neural networks. Deep learning approaches have the in-built capability to automatically learn optimal features from original input signal [185]. Therefore, the time consumed by the feature extraction process in other feature engineering is canceled. Most DL systems rely on training and verification data sets that are annotated by humans.

The potential offered by DL in power system analysis is still under investigation. Indeed, the automatic features extraction and the high pattern recognition capability of these approaches pave the way for an extensive use for power system issue prediction, detection and estimation. Hence, the last years have witnessed a big interest of researchers in the field of power system monitoring for deep learning as a medium for power quality enhancement and disturbancesmitigation [145,186–190]. Hence, in [191], an unsupervised deep learning technique has been investigated for load profile management and classification. In [192], a convolutional neural network has been proposed for direct load control of a heterogeneous cluster of residential load. Moreover, in [193], authors have proposed a voltage sag estimation approach based on a deep convolutional neural network. Specifically, the paper presents an approach that allowed to estimate voltage sag parameters for

unmonitored buses in a grid regardless of the power system operating conditions, fault characteristics and location.

4.3. Critical Analysis and Future Research Topics and Challenges

The choice of an appropriate machine learning approach for decision making is not an easy task. Indeed, the application of machine learning for PQ monitoring requires experts both in electrical engineering and machine learning technology. Experts will allow addressing issues related to the complexity of the PQ disturbances to deal with the choice of adequate measurement devices and the machine learning technique benchmarking and tuning. Even though these technologies offer many opportunities that allow enhancing the diagnosis reliability and effectiveness, it suffers from several drawbacks. Indeed, the main drawback of machine learning techniques is the initial training stage, which requires a large set of measurement databases for different PQ disturbances and various operating conditions. This stage is critical for optimal operation and requires relatively high computational effort. The black-box behavior of such approaches may be misleading or produce results limited to a set of systems. Moreover, the performance of the machine learning approaches depends on the selection of appropriate feature extraction techniques.

Dealing with PQ disturbance detection and classification is a topic of great interest for both academia and industry. Some issues are still open and worth further investigations, such as the high-performance data processing technologies and analysis techniques for intelligent decision-making in large-scale complex multi-energy systems, lightweight machine learning-based solutions for fast classification, and so forth. It has been recently suggested that quality of service (QoS) application requirements could be met considering emerging new sensing technologies and embedded computing [61]. Moreover, in a smart grid context, where hybrid energy systems interact with other system architectures at different application levels, the use of advanced computing and communication technologies, e.g., edge computing, ubiquitous Internet of Things and 5G wireless networks, will obviously improve the monitoring of smart grid conditions.

5. Conclusions and Prospects

This paper has reviewed the main approaches used for power quality monitoring in smart grids. Two aspects have been taken into consideration, which are the feature extraction techniques and classification and decision making approaches. Attempts have been made to highlight current trends for PQ analysis based on advanced signal processing and machine learning. An accurate choice of signal processing techniques for fault detection and characteristic determination is a challenging issue. In fact, in transient, off-nominal conditions, and under nonstationary operating conditions (flicker, spikes, notching, etc.), a short data acquisition time is required, which affects the frequency estimate resolution and amplitude estimate accuracy. Moreover, in a three-phase power grid, the electrical signals (voltages and currents) are multi-dimensional in nature, which should be exploited to enhance the statistical performance of fault feature extraction. It is highlighted that despite the rich literature, the choice of a particular technique is not an easy task since several parameters must be taken into account, which requires an expert of PQ monitoring for appropriate analysis.

PQ disturbance monitoring requires post-processing algorithms to determine fault characteristics (starting and ending time, duration, etc.), fault types, causes and potential action that could be taken. Machine learning techniques have been widely investigated in the last ten years for PQ monitoring and event classification. These include several sophisticated algorithms such as support vector machine, artificial neural networks, fuzzy expert systems, and many others. It is demonstrated that these approaches can effectively deal with a huge amount of data issued from all sensors and PMUs on the power grid and consequently improve the diagnosis procedure while taking benefits from previous power grid events and disturbances.

Author Contributions: Conceptualization, E.E., M.F.Z. and M.B.; methodology, E.E., M.F.Z. and M.B.; validation, E.E., M.F.Z., M.B. and S.E.H.; formal analysis, E.E., M.F.Z., M.B. and S.E.H.; investigation, E.E., M.F.Z., M.B. and S.E.H.; resources, E.E., M.F.Z., M.B. and S.E.H.; data curation, E.E., M.F.Z., M.B. and S.E.H.; writing—original draft preparation, E.E.; writing—review and editing, E.E., M.F.Z., M.B. and S.E.H.; visualization, E.E., M.F.Z., M.B. and S.E.H.; supervision, E.E., M.F.Z., M.B. and S.E.H.; project administration, E.E.; funding acquisition, E.E. All authors have read and agreed to the published version of the manuscript.

Funding: This research received no external funding.

Conflicts of Interest: The authors declare no conflict of interest.

Abbreviations

The following abbreviations are used in this manuscript:

PQ	Power Quality
PMU	Phasor Measurement Unit
DSP	Digital Signal Processing
IoT	Internet of Things
MLE	Maximum Likelihood Estimation
MUSIC	Multiple Signal Classification
ESPRIT	Estimation of Signal Parameters via Rotational Invariance Techniques
ARMA	AutoRegressive Moving Average
EMD	Empirical Mode Decomposition
DWT	Discrete Wavelet transform
ANN	Artificial Neural Network
SVM	Support Vector Machine
CNN	Convolution Neural Network
RNN	Recurrent Neural Network
I-RNN	Identity-Recurrent Neural Network
LSTM	Long Short-Term Memory
GRU	Gated Recurrent Units
CNN-LSTM	Convolutional Neural Network-Long Short-Term Memory
AI	Artificial Intelligence
SCADA	Supervisory Control and Data Acquisition
GPS	Global Positioning System
PDC	Phasor Data Concentrator
CCN	Central Control Network
IEC	International Electrotechnical Commission
IEEE	Institute of Electrical and Electronics Engineers
TVE	Total Vector Error
RMS	Root Mean Square
PSD	Power Spectral Density
FFT	Fast Fourier Transform
DTFT	Discrete Time Fourier transform
SVD	Singular Value Decomposition
EVD	EigenValues Decomposition
SNR	Signal to Noise Ratio
IF	Instantaneous Frequency
IAm	Instantaneous Amplitude
TEO	Teager energy operator
ESA	Energy Separation Algorithm
CT	Concordia Transform
PCA	Principal Component Analysis
STFT	Short-Time Fourier Transform
CWT	Continuous Wavelet Transform
WVD	Wigner–Ville Distribution

HHT	Hilbert–Huang Transform
HAS	Hilbert Spectral Analysis
IMF	Intrinsic Mode Function
VMD	Variational Mode Decomposition
EEMD	Ensemble EMD
SD	Synchronous Demodulator
ROCOF	Rate Of Change Of Frequency
MLP	Multilayer Perceptron
DL	Deep Learning
QoS	Quality of Service
SCADA	Supervisory Control And Data Acquisition
WAMS	Wide Area Measurement System
IpDFT	Interpolated Discrete Fourier Transform
DCF	Down-Conversion and low-pass Filtering
TFT	Taylor Fourier Transform

References

1. Ekanayake, J.B.; Jenkins, N.; Liyanage, K.; Wu, J.; Yokoyama, A. *Smart Grid: Technology and Applications*; John Wiley & Sons: Chichester, UK, 2012.
2. Fang, X.; Misra, S.; Xue, G.; Yang, D. Smart grid—The new and improved power grid: A survey. *IEEE Commun. Surv. Tutor.* **2011**, *14*, 944–980. [CrossRef]
3. Gungor, V.C.; Sahin, D.; Kocak, T.; Ergut, S.; Buccella, C.; Cecati, C.; Hancke, G.P. A survey on smart grid potential applications and communication requirements. *IEEE Trans. Ind. Inform.* **2012**, *9*, 28–42. [CrossRef]
4. Gungor, V.C.; Sahin, D.; Kocak, T.; Ergut, S.; Buccella, C.; Cecati, C.; Hancke, G.P. Smart grid technologies: Communication technologies and standards. *IEEE Trans. Ind. Inform.* **2011**, *7*, 529–539. [CrossRef]
5. Mwasilu, F.; Justo, J.J.; Kim, E.K.; Do, T.D.; Jung, J.W. Electric vehicles and smart grid interaction: A review on vehicle to grid and renewable energy sources integration. *Renew. Sustain. Energy Rev.* **2014**, *34*, 501–516. [CrossRef]
6. Phuangpornpitak, N.; Tia, S. Opportunities and challenges of integrating renewable energy in smart grid system. *Energy Procedia* **2013**, *34*, 282–290. [CrossRef]
7. Elbouchikhi, E.; Feld, G.; Amirat, Y.; Benbouzid, M.; Le Gall, F. Design and experimental implementation of a wind energy conversion platform with education and research capabilities. *Comput. Electr. Eng.* **2020**, *85*, 106661. [CrossRef]
8. Mortaji, H.; Ow, S.H.; Moghavvemi, M.; Almurib, H.A.F. Load shedding and smart-direct load control using internet of things in smart grid demand response management. *IEEE Trans. Ind. Appl.* **2017**, *53*, 5155–5163. [CrossRef]
9. Hui, H.; Ding, Y.; Shi, Q.; Li, F.; Song, Y.; Yan, J. 5G network-based Internet of Things for demand response in smart grid: A survey on application potential. *Appl. Energy* **2020**, *257*, 113972. [CrossRef]
10. Mortaji, H.; Hock, O.S.; Moghavvemi, M.; Almurib, H.A. Smart grid demand response management using internet of things for load shedding and smart-direct load control. In Proceedings of the 2016 IEEE Industry Applications Society Annual Meeting, Portland, OR, USA, 2–6 October 2016; pp. 1–7.
11. Kabalci, Y. A survey on smart metering and smart grid communication. *Renew. Sustain. Energy Rev.* **2016**, *57*, 302–318. [CrossRef]
12. Keshtkar, A.; Arzanpour, S. An adaptive fuzzy logic system for residential energy management in smart grid environments. *Appl. Energy* **2017**, *186*, 68–81. [CrossRef]
13. Zhao, C.; He, J.; Cheng, P.; Chen, J. Consensus-based energy management in smart grid with transmission losses and directed communication. *IEEE Trans. Smart Grid* **2016**, *8*, 2049–2061. [CrossRef]
14. Worighi, I.; Maach, A.; Hafid, A.; Hegazy, O.; Van Mierlo, J. Integrating renewable energy in smart grid system: Architecture, virtualization and analysis. *Sustain. Energy Grids Netw.* **2019**, *18*, 100226. [CrossRef]
15. Yang, K.; Walid, A. Outage-storage tradeoff in frequency regulation for smart grid with renewables. *IEEE Trans. Smart Grid* **2013**, *4*, 245–252. [CrossRef]
16. Standard British. Voltage Characteristics of Electricity Supplied by Public Distribution Networks. October 2007. Available online: https://webstore.ansi.org/standards/bsi/bsen501602007 (accessed on 21 September 2007).
17. International Standard. Testing and Measurement Techniques—Power Quality Measurement Methods. March 2021. Available online: https://webstore.iec.ch/publication/68642 (accessed on 13 October 2021).
18. *IEEE Recommended Practice for Monitoring Electric Power Quality*; IEEE 1159-2019 (Revision of IEEE Standard 1159-2009); 13 August 2019. Available online: https://ieeexplore.ieee.org/document/8796486 (accessed on 13 October 2021). [CrossRef]
19. Fuchs, E.; Masoum, M.A. *Power Quality in Power Systems and Electrical Machines*; Academic Press: Cambridge, MA, USA, 2011.
20. Bollen, M.H. What is power quality? *Electr. Power Syst. Res.* **2003**, *66*, 5–14. [CrossRef]
21. Kusko, A. *Power Quality in Electrical Systems*; McGraw-Hill Education: New York, NY, USA, 2007.
22. Mishra, S.; Bhende, C.; Panigrahi, B. Detection and classification of power quality disturbances using S-transform and probabilistic neural network. *IEEE Trans. Power Deliv.* **2007**, *23*, 280–287. [CrossRef]
23. Bollen, M.H.; Gu, I.Y. *Signal Processing of Power Quality Disturbances*; John Wiley & Sons: Hoboken, NJ, USA, 2006; Volume 30.

24. Muscas, C. Power quality monitoring in modern electric distribution systems. *IEEE Instrum. Meas. Mag.* **2010**, *13*, 19–27. [CrossRef]
25. Elphick, S.; Ciufo, P.; Drury, G.; Smith, V.; Perera, S.; Gosbell, V. Large scale proactive power-quality monitoring: An example from Australia. *IEEE Trans. Power Deliv.* **2016**, *32*, 881–889. [CrossRef]
26. Parle, J.; Madrigal, M.; Acha, E. Trends in power quality monitoring. *IEEE Power Eng. Rev.* **2001**, *21*, 3–21. [CrossRef]
27. Yildirim, O.; Eristi, B.; Eristi, H.; Unal, S.; Erol, Y.; Demir, Y. FPGA-based online power quality monitoring system for electrical distribution network. *Measurement* **2018**, *121*, 109–121. [CrossRef]
28. Venkatraman, K.; Reddy, B.D.; Selvan, M.; Moorthi, S.; Kumaresan, N.; Gounden, N.A. Online condition monitoring and power management system for standalone micro-grid using FPGAs. *IET Gener. Transm. Distrib.* **2016**, *10*, 3875–3884. [CrossRef]
29. Nilsson, J.; Bertling, L. Maintenance management of wind power systems using condition monitoring systems—Life cycle cost analysis for two case studies. *IEEE Trans. Energy Convers.* **2007**, *22*, 223–229. [CrossRef]
30. Liu, J.; Tang, J.; Ponci, F.; Monti, A.; Muscas, C.; Pegoraro, P.A. Trade-offs in PMU deployment for state estimation in active distribution grids. *IEEE Trans. Smart Grid* **2012**, *3*, 915–924. [CrossRef]
31. IEEE/IEC. *International Standard—Measuring Relays and Protection Equipment—Part 118-1: Synchrophasor for Power Systems Measurements*; IEC/IEEE 60255-118-1:2018; 19 December 2018. Available online: https://standards.ieee.org/standard/60255-118-1-2018.html (accessed on 13 October 2021).
32. Tai, X.; Marelli, D.; Rohr, E.; Fu, M. Optimal PMU placement for power system state estimation with random component outages. *Int. J. Electr. Power Energy Syst.* **2013**, *51*, 35–42. [CrossRef]
33. Bashian, A.; Assili, M.; Anvari-Moghaddam, A. A security-based observability method for optimal PMU-sensor placement in WAMS. *Int. J. Electr. Power Energy Syst.* **2020**, *121*, 106157. [CrossRef]
34. Bashian, A.; Assili, M.; Anvari-Moghaddam, A.; Catalão, J.P.S. Optimal Design of a Wide Area Measurement System Using Hybrid Wireless Sensors and Phasor Measurement Units. *Electronics* **2019**, *8*, 1085. [CrossRef]
35. Macii, D.; Belega, D.; Petri, D. IpDFT-Tuned Estimation Algorithms for PMUs: Overview and Performance Comparison. *Appl. Sci.* **2021**, *11*, 2318. [CrossRef]
36. Belega, D.; Fontanelli, D.; Petri, D. Low-complexity least-squares dynamic synchrophasor estimation based on the discrete Fourier transform. *IEEE Trans. Instrum. Meas.* **2015**, *64*, 3284–3296. [CrossRef]
37. Singh, A.K.; Pal, B.C. Rate of change of frequency estimation for power systems using interpolated DFT and Kalman filter. *IEEE Trans. Power Syst.* **2019**, *34*, 2509–2517. [CrossRef]
38. Macii, D.; Petri, D. Digital filters for phasor measurement units: Design criteria, advantages and limitations. In Proceedings of the 2019 IEEE 10th International Workshop on Applied Measurements for Power Systems (AMPS), Aachen, Germany, 25–27 September 2019; pp. 1–6.
39. Kamwa, I.; Samantaray, S.; Joos, G. Wide frequency range adaptive phasor and frequency PMU algorithms. *IEEE Trans. Smart Grid* **2013**, *5*, 569–579. [CrossRef]
40. Zhan, L.; Liu, Y.; Liu, Y. A Clarke transformation-based DFT phasor and frequency algorithm for wide frequency range. *IEEE Trans. Smart Grid* **2016**, *9*, 67–77. [CrossRef]
41. Xia, T.; Liu, Y. Single-phase phase angle measurements in electric power systems. *IEEE Trans. Power Syst.* **2009**, *25*, 844–852. [CrossRef]
42. Kang, S.H.; Lee, D.G.; Nam, S.R.; Crossley, P.A.; Kang, Y.C. Fourier transform-based modified phasor estimation method immune to the effect of the DC offsets. *IEEE Trans. Power Deliv.* **2009**, *24*, 1104–1111. [CrossRef]
43. Derviškadić, A.; Romano, P.; Paolone, M. Iterative-interpolated DFT for synchrophasor estimation: A single algorithm for P- and M-class compliant PMUs. *IEEE Trans. Instrum. Meas.* **2017**, *67*, 547–558. [CrossRef]
44. Petri, D.; Fontanelli, D.; Macii, D. A frequency-domain algorithm for dynamic synchrophasor and frequency estimation. *IEEE Trans. Instrum. Meas.* **2014**, *63*, 2330–2340. [CrossRef]
45. Huang, C.; Xie, X.; Jiang, H. Dynamic phasor estimation through DSTKF under transient conditions. *IEEE Trans. Instrum. Meas.* **2017**, *66*, 2929–2936. [CrossRef]
46. Nanda, S.; Dash, P.K. A Gauss–Newton ADALINE for dynamic phasor estimation of power signals and its FPGA implementation. *IEEE Trans. Instrum. Meas.* **2016**, *67*, 45–56. [CrossRef]
47. De la O Serna, J.A.; Rodriguez-Maldonado, J. Instantaneous oscillating phasor estimates with Taylor K-Kalman filters. *IEEE Trans. Power Syst.* **2011**, *26*, 2336–2344. [CrossRef]
48. Zečević, Ž.; Krstajić, B.; Popović, T. Improved frequency estimation in unbalanced three-phase power system using coupled orthogonal constant modulus algorithm. *IEEE Trans. Power Deliv.* **2016**, *32*, 1809–1816. [CrossRef]
49. Messina, F.; Marchi, P.; Vega, L.R.; Galarza, C.G.; Laiz, H. A novel modular positive-sequence synchrophasor estimation algorithm for PMUs. *IEEE Trans. Instrum. Meas.* **2016**, *66*, 1164–1175. [CrossRef]
50. Vejdan, S.; Sanaye-Pasand, M.; Malik, O.P. Accurate dynamic phasor estimation based on the signal model under off-nominal frequency and oscillations. *IEEE Trans. Smart Grid* **2015**, *8*, 708–719. [CrossRef]
51. Chauhan, K.; Reddy, M.V.; Sodhi, R. A novel distribution-level phasor estimation algorithm using empirical wavelet transform. *IEEE Trans. Ind. Electron.* **2018**, *65*, 7984–7995. [CrossRef]
52. Narduzzi, C.; Bertocco, M.; Frigo, G.; Giorgi, G. Fast-TFM—Multifrequency phasor measurement for distribution networks. *IEEE Trans. Instrum. Meas.* **2018**, *67*, 1825–1835. [CrossRef]

53. Chen, L.; Zhao, W.; Wang, Q.; Wang, F.; Huang, S. Dynamic harmonic synchrophasor estimator based on sinc interpolation functions. *IEEE Trans. Instrum. Meas.* **2018**, *68*, 3054–3065. [CrossRef]
54. Zečević, Ž.; Jokić, I.; Popović, T.; Krstajić, B. An efficient phasor and frequency estimation algorithm for wide frequency range. *Electr. Power Syst. Res.* **2020**, *180*, 106124. [CrossRef]
55. Song, J.; Zhang, J.; Wen, H. Accurate Dynamic Phasor Estimation by Matrix Pencil and Taylor Weighted Least Squares Method. *IEEE Trans. Instrum. Meas.* **2021**, *70*, 1–11.
56. Xu, S.; Liu, H.; Bi, T.; Martin, K. An improved Taylor weighted least squares method for estimating synchrophasor. *Int. J. Electr. Power Energy Syst.* **2020**, *120*, 105987. [CrossRef]
57. Mahela, O.P.; Shaik, A.G.; Gupta, N. A critical review of detection and classification of power quality events. *Renew. Sustain. Energy Rev.* **2015**, *41*, 495–505. [CrossRef]
58. Tu, C.; He, X.; Shuai, Z.; Jiang, F. Big data issues in smart grid—A review. *Renew. Sustain. Energy Rev.* **2017**, *79*, 1099–1107. [CrossRef]
59. Mishra, M. Power quality disturbance detection and classification using signal processing and soft computing techniques: A comprehensive review. *Int. Trans. Electr. Energy Syst.* **2019**, *29*, e12008. [CrossRef]
60. Hossain, E.; Khan, I.; Un-Noor, F.; Sikander, S.S.; Sunny, M.S.H. Application of big data and machine learning in smart grid, and associated security concerns: A review. *IEEE Access* **2019**, *7*, 13960–13988. [CrossRef]
61. Rivas, A.E.L.; Abrão, T. Faults in smart grid systems: Monitoring, detection and classification. *Electr. Power Syst. Res.* **2020**, *189*, 106602. [CrossRef]
62. Khetarpal, P.; Tripathi, M.M. A critical and comprehensive review on power quality disturbance detection and classification. *Sustain. Comput. Inform. Syst.* **2020**, *28*, 100417.
63. Ibrahim, M.S.; Dong, W.; Yang, Q. Machine learning driven smart electric power systems: Current trends and new perspectives. *Appl. Energy* **2020**, *272*, 115237. [CrossRef]
64. Chawda, G.S.; Shaik, A.G.; Shaik, M.; Padmanaban, S.; Holm-Nielsen, J.B.; Mahela, O.P.; Kaliannan, P. Comprehensive review on detection and classification of power quality disturbances in utility grid with renewable energy penetration. *IEEE Access* **2020**, *8*, 146807–146830. [CrossRef]
65. Gargoom, A.M.; Ertugrul, N.; Soong, W. A comparative study on effective signal processing tools for power quality monitoring. In Proceedings of the 2005 European Conference on Power Electronics and Applications, Dresden, Germany, 11–14 September 2005. [CrossRef]
66. Karasu, S.; Saraç, Z. Classification of power quality disturbances by 2D-Riesz Transform, multi-objective grey wolf optimizer and machine learning methods. *Digit. Signal Process.* **2020**, *101*, 102711. [CrossRef]
67. Khokhar, S.; Zin, A.A.B.M.; Mokhtar, A.S.B.; Pesaran, M. A comprehensive overview on signal processing and artificial intelligence techniques applications in classification of power quality disturbances. *Renew. Sustain. Energy Rev.* **2015**, *51*, 1650–1663. [CrossRef]
68. Yilmaz, A.S.; Alkan, A.; Asyali, M.H. Applications of parametric spectral estimation methods on detection of power system harmonics. *Electr. Power Syst. Res.* **2008**, *78*, 683–693. [CrossRef]
69. Zolfaghari, R.; Shrivastava, Y.; Agelidis, V.G.; Chu, G.L. Using windowed ESPRIT spectral estimation for measuring power quality indices. In Proceedings of the 2010 IEEE PES Innovative Smart Grid Technologies Conference Europe (ISGT Europe), Gothenburg, Sweden, 11–13 October 2010; pp. 1–8.
70. Zygarlicki, J.; Mroczka, J. Variable-frequency Prony method in the analysis of electrical power quality. *Metrol. Meas. Syst.* **2012**, *19*, 39–48. [CrossRef]
71. Liu, X.; Liu, C.; Wang, J.; Xing, J. Inter-harmonic parameter estimation based on FFT and MUSIC. *Power Syst. Prot. Control* **2009**, *5*, 12–15.
72. Kapoor, R.; Saini, M.K. Hybrid demodulation concept and harmonic analysis for single/multiple power quality events detection and classification. *Int. J. Electr. Power Energy Syst.* **2011**, *33*, 1608–1622. [CrossRef]
73. Jayasree, T.; Devaraj, D.; Sukanesh, R. Power quality disturbance classification using Hilbert transform and RBF networks. *Neurocomputing* **2010**, *73*, 1451–1456. [CrossRef]
74. Senroy, N.; Suryanarayanan, S.; Ribeiro, P.F. An improved Hilbert–Huang method for analysis of time-varying waveforms in power quality. *IEEE Trans. Power Syst.* **2007**, *22*, 1843–1850. [CrossRef]
75. Liu, J.; Song, H.; Sun, H.; Zhao, H. High-Precision Identification of Power Quality Disturbances Under Strong Noise Environment Based on FastICA and Random Forest. *IEEE Trans. Ind. Inform.* **2020**, *17*, 377–387. [CrossRef]
76. Ucar, F.; Alcin, O.F.; Dandil, B.; Ata, F. Power quality event detection using a fast extreme learning machine. *Energies* **2018**, *11*, 145. [CrossRef]
77. Masoum, M.; Jamali, S.; Ghaffarzadeh, N. Detection and classification of power quality disturbances using discrete wavelet transform and wavelet networks. *IET Sci. Meas. Technol.* **2010**, *4*, 193–205. [CrossRef]
78. Jiang, H.; Zhang, J.J.; Gao, W.; Wu, Z. Fault detection, identification, and location in smart grid based on data-driven computational methods. *IEEE Trans. Smart Grid* **2014**, *5*, 2947–2956. [CrossRef]
79. Thirumala, K.; Umarikar, A.C.; Jain, T. Estimation of single-phase and three-phase power-quality indices using empirical wavelet transform. *IEEE Trans. Power Deliv.* **2014**, *30*, 445–454. [CrossRef]
80. Adamo, F.; Attivissimo, F.; Di Nisio, A.; Savino, M.; Spadavecchia, M. A spectral estimation method for nonstationary signals analysis with application to power systems. *Measurement* **2015**, *73*, 247–261. [CrossRef]

81. Xu, S.; Liu, H.; Bi, T. A novel frequency estimation method based on complex Bandpass filters for P-class PMUs with short reporting latency. *IEEE Trans. Power Deliv.* **2020**. [CrossRef]
82. Tosato, P.; Macii, D.; Luiso, M.; Brunelli, D.; Gallo, D.; Landi, C. A tuned lightweight estimation algorithm for low-cost phasor measurement units. *IEEE Trans. Instrum. Meas.* **2018**, *67*, 1047–1057. [CrossRef]
83. Bollen, M.H.; Zhang, L. Different methods for classification of three-phase unbalanced voltage dips due to faults. *Electr. Power Syst. Res.* **2003**, *66*, 59–69. [CrossRef]
84. Bollen, M.H. Algorithms for characterizing measured three-phase unbalanced voltage dips. *IEEE Trans. Power Deliv.* **2003**, *18*, 937–944. [CrossRef]
85. Sahani, M.; Dash, P.K. Automatic power quality events recognition based on Hilbert Huang transform and weighted bidirectional extreme learning machine. *IEEE Trans. Ind. Inform.* **2018**, *14*, 3849–3858. [CrossRef]
86. Lee, C.; Nam, S. Efficient feature vector extraction for automatic classification of power quality disturbances. *Electron. Lett.* **1998**, *34*, 1059–1061. [CrossRef]
87. Monedero, I.; Leon, C.; Ropero, J.; Garcia, A.; Elena, J.M.; Montano, J.C. Classification of electrical disturbances in real time using neural networks. *IEEE Trans. Power Deliv.* **2007**, *22*, 1288–1296. [CrossRef]
88. Valtierra-Rodriguez, M.; de Jesus Romero-Troncoso, R.; Osornio-Rios, R.A.; Garcia-Perez, A. Detection and classification of single and combined power quality disturbances using neural networks. *IEEE Trans. Ind. Electron.* **2013**, *61*, 2473–2482. [CrossRef]
89. Bhende, C.; Mishra, S.; Panigrahi, B. Detection and classification of power quality disturbances using S-transform and modular neural network. *Electr. Power Syst. Res.* **2008**, *78*, 122–128. [CrossRef]
90. Ekici, S. Classification of power system disturbances using support vector machines. *Expert Syst. Appl.* **2009**, *36*, 9859–9868. [CrossRef]
91. Lin, W.M.; Wu, C.H.; Lin, C.H.; Cheng, F.S. Detection and classification of multiple power-quality disturbances with wavelet multiclass SVM. *IEEE Trans. Power Deliv.* **2008**, *23*, 2575–2582. [CrossRef]
92. Liu, Z.; Cui, Y.; Li, W. A classification method for complex power quality disturbances using EEMD and rank wavelet SVM. *IEEE Trans. Smart Grid* **2015**, *6*, 1678–1685. [CrossRef]
93. Erişti, H.; Uçar, A.; Demir, Y. Wavelet-based feature extraction and selection for classification of power system disturbances using support vector machines. *Electr. Power Syst. Res.* **2010**, *80*, 743–752. [CrossRef]
94. Yang, H.; Liu, X.; Zhang, D.; Chen, T.; Li, C.; Huang, W. Machine learning for power system protection and control. *Electr. J.* **2021**, *34*, 106881. [CrossRef]
95. Wang, H.; Lei, Z.; Zhang, X.; Zhou, B.; Peng, J. A review of deep learning for renewable energy forecasting. *Energy Convers. Manag.* **2019**, *198*, 111799. [CrossRef]
96. Fernandes, R.A.S.; da Silva, I.N.; Oleskovicz, M. Load profile identification interface for consumer online monitoring purposes in smart grids. *IEEE Trans. Ind. Inform.* **2012**, *9*, 1507–1517. [CrossRef]
97. Oubrahim, Z.; Choqueuse, V.; Amirat, Y.; Benbouzid, M.E.H. Disturbances classification based on a model order selection method for power quality monitoring. *IEEE Trans. Ind. Electron.* **2017**, *64*, 9421–9432. [CrossRef]
98. Ignatova, V.; Granjon, P.; Bacha, S. Space vector method for voltage dips and swells analysis. *IEEE Trans. Power Deliv.* **2009**, *24*, 2054–2061. [CrossRef]
99. Bollen, M.H. Understanding power quality problems. In *Voltage Sags and Interruptions*; IEEE Press: Piscataway, NJ, USA, 2000.
100. Dahal, O.P.; Brahma, S.M.; Cao, H. Comprehensive clustering of disturbance events recorded by phasor measurement units. *IEEE Trans. Power Deliv.* **2013**, *29*, 1390–1397. [CrossRef]
101. Saini, M.K.; Kapoor, R. Classification of power quality events–a review. *Int. J. Electr. Power Energy Syst.* **2012**, *43*, 11–19. [CrossRef]
102. Oubrahim, Z. On Electric Grid Power Quality Monitoring Using Parametric Signal Processing Techniques. Ph.D. Thesis, Thèse de Doctorat de l'Université de Bretagne Occidentale, Brest, France, November 2017.
103. De Almeida, A.; Moreira, L.; Delgado, J. Power quality problems and new solutions. In Proceedings of the International Conference on Renewable Energies and Power Quality, Vigo, Spain, 9–11 April 2003; Volume 3.
104. Bollen, M.H.; Gu, I.Y.; Santoso, S.; McGranaghan, M.F.; Crossley, P.A.; Ribeiro, M.V.; Ribeiro, P.F. Bridging the gap between signal and power. *IEEE Signal Process. Mag.* **2009**, *26*, 12–31. [CrossRef]
105. Monti, A.; Muscas, C.; Ponci, F. *Phasor Measurement Units and Wide Area Monitoring Systems*; Academic Press: Cambridge, MA, USA, 2016.
106. Chakrabarti, S.; Kyriakides, E. Optimal placement of phasor measurement units for power system observability. *IEEE Trans. Power Syst.* **2008**, *23*, 1433–1440. [CrossRef]
107. Tholomier, D.; Kang, H.; Cvorovic, B. Phasor measurement units: Functionality and applications. In Proceedings of the 2009 Power Systems Conference, Clemson, SC, USA, 10–13 March 2009; pp. 1–12.
108. Singh, B.; Sharma, N.; Tiwari, A.; Verma, K.; Singh, S. Applications of phasor measurement units (PMUs) in electric power system networks incorporated with FACTS controllers. *Int. J. Eng. Sci. Technol.* **2011**, *3*. [CrossRef]
109. Khan, R.H.; Khan, J.Y. A comprehensive review of the application characteristics and traffic requirements of a smart grid communications network. *Comput. Netw.* **2013**, *57*, 825–845. [CrossRef]
110. Radulović, M.; Zečević, Ž.; Krstajić, B. Dynamic phasor estimation by symmetric Taylor weighted least square filter. *IEEE Trans. Power Deliv.* **2019**, *35*, 828–836. [CrossRef]

111. Belega, D.; Fontanelli, D.; Petri, D. Dynamic phasor and frequency measurements by an improved Taylor weighted least squares algorithm. *IEEE Trans. Instrum. Meas.* **2015**, *64*, 2165–2178. [CrossRef]
112. Ferrero, R.; Pegoraro, P.A.; Toscani, S. Synchrophasor Estimation for Three-Phase Systems Based on Taylor Extended Kalman Filtering. *IEEE Trans. Instrum. Meas.* **2020**, *69*, 6723–6730. [CrossRef]
113. Fan, L.; Wehbe, Y. Extended Kalman filtering based real-time dynamic state and parameter estimation using PMU data. *Electr. Power Syst. Res.* **2013**, *103*, 168–177. [CrossRef]
114. De la O Serna, J.A.; Rodríguez-Maldonado, J. Taylor–Kalman–Fourier filters for instantaneous oscillating phasor and harmonic estimates. *IEEE Trans. Instrum. Meas.* **2012**, *61*, 941–951. [CrossRef]
115. Kay, S. *Modern Spectral Estimation: Theory and Application*; Prentice Hall, Englewood Cliffs: Hoboken, NJ, USA, 1998.
116. Ribeiro, P.F.; Duque, C.A.; Ribeiro, P.M.; Cerqueira, A.S. *Power Systems Signal Processing for Smart Grids*; John Wiley & Sons: Hoboken, NJ, USA, 2013.
117. Kay, S.; Marple, S. Spectrum Analysis—A Modern Perspective. *Proc. IEEE* **1981**, *69*, 1380–1419. [CrossRef]
118. Alkan, A.; Yilmaz, A.S. Frequency domain analysis of power system transients using Welch and Yule–Walker AR methods. *Energy Convers. Manag.* **2007**, *48*, 2129–2135. [CrossRef]
119. Romano, P.; Paolone, M. Enhanced interpolated-DFT for synchrophasor estimation in FPGAs: Theory, implementation, and validation of a PMU prototype. *IEEE Trans. Instrum. Meas.* **2014**, *63*, 2824–2836. [CrossRef]
120. Belega, D.; Petri, D. Fast procedures for accurate parameter estimation of sine-waves affected by noise and harmonic distortion. *Digit. Signal Process.* **2021**, *114*, 103035. [CrossRef]
121. Belega, D.; Petri, D. Accuracy analysis of the multicycle synchrophasor estimator provided by the interpolated DFT algorithm. *IEEE Trans. Instrum. Meas.* **2013**, *62*, 942–953. [CrossRef]
122. Stoica, P.; Moses, R.L. *Introduction to Spectral Analysis*; Prentice-Hall: Hoboken, NJ, USA, 1997.
123. Elbouchikhi, E.; Choqueuse, V.; Benbouzid, M. Induction machine diagnosis using stator current advanced signal processing. *Int. J. Energy Convers.* **2015**, *3*, 76–87.
124. Stoica, P.; Selen, Y. Model-order selection: A review of information criterion rules. *IEEE Signal Process. Mag.* **2004**, *21*, 36–47. [CrossRef]
125. Stoica, P.; Nehorai, A. MUSIC, Maximum Likelihood, and Cramer-Rao Bound. *IEEE Trans. Acoust. Speech Signal Process.* **1989**, *37*, 720–741. [CrossRef]
126. Zhang, S.; Luo, R.C.; Hu, Z.Y.; Huang, B. Root-MUSIC and Prony based parameter estimation of voltage flicker. *J. Electr. Power Sci. Technol.* **2013**, *4*, 43–48.
127. Zolfaghari, R.; Shrivastava, Y.; Agelidis, V.G. Evaluation of windowed ESPRIT virtual instrument for estimating Power Quality Indices. *Electr. Power Syst. Res.* **2012**, *83*, 58–65. [CrossRef]
128. Kay, S. *Fundamentals of Statistical Signal Processing: Estimation Theory*; Signal Processing Series; 17th Printing; Prentice-Hall: Upper Saddle River, NJ, USA, 26 March 1993.
129. Oubrahim, Z.; Choqueuse, V.; Amirat, Y.; Benbouzid, M.E.H. Maximum-likelihood frequency and phasor estimations for electric power grid monitoring. *IEEE Trans. Ind. Inform.* **2017**, *14*, 167–177. [CrossRef]
130. Elbouchikhi, E.; Choqueuse, V.; Benbouzid, M. Induction machine faults detection using stator current parametric spectral estimation. *Mech. Syst. Signal Process.* **2015**, *52*, 447–464. [CrossRef]
131. Elbouchikhi, E.; Choqueuse, V.; Benbouzid, M. Condition monitoring of induction motors based on stator currents demodulation. *Int. Rev. Electr.-Eng.—IREE* **2015**, *10*, 704–715. [CrossRef]
132. Vakman, D. On the analytic signal, the Teager-Kaiser energy algorithm, and other methods for defining amplitude and frequency. *Signal Process. IEEE Trans.* **1996**, *44*, 791–797. [CrossRef]
133. Wang, J.; Liu, H.; Xiao, H. An approach to measure interharmonics-flicker based on synchronous demodulation. *Proc. CSEE* **2011**, *31*, 67–72.
134. Hahn, S.L. *Hilbert Transforms in Signal Processing*; Artech House: Norwell, MA, USA, 1996.
135. Oppenheim, A.; Schafer, R.; Padgett, W. *Discrete-Time Signal Processing*, 3rd ed.; Prentice Hall: Hoboken, NJ, USA, 2009.
136. Picinbono, B. On instantaneous amplitude and phase of signals. *IEEE Trans. Signal Process.* **1997**, *45*, 552–560. [CrossRef]
137. Boashash, B. Time-Frequency Signal Analysis. In *Advances in Spectrum Estimation*; Haykin, S., Ed.; Engewood Cliffs, Prentice-Hall: Hoboken, NJ, USA, 1991.
138. Marple, L., Jr. Computing the discrete-time "analytic" signal via FFT. *Signal Process. IEEE Trans.* **1999**, *47*, 2600–2603. [CrossRef]
139. Maragos, P.; Kaiser, J.; Quatieri, T. Energy Separation in Signal Modulations with Application to Speech Analysis. *IEEE Trans. Signal Process.* **1993**, *10*, 3024–3051. [CrossRef]
140. Maragos, P.; Kaiser, J.; Quartieri, T. On Amplitude and Frequency Demodulation Using Energy Operators. *IEEE Trans. Signal Process.* **1993**, *41*, 1532–1550. [CrossRef]
141. Subasi, A.; Yilmaz, A.S.; Tufan, K. Detection of generated and measured transient power quality events using Teager Energy Operator. *Energy Convers. Manag.* **2011**, *52*, 1959–1967. [CrossRef]
142. Cho, S.H.; Hur, J.; Chung, I.Y. An applicability of teager energy operator and energy separation algorithm for waveform distortion analysis: Harmonics, inter-harmonics and frequency variation. *J. Electr. Eng. Technol.* **2014**, *9*, 1210–1216. [CrossRef]
143. Aller, J.M.; Bueno, A.; Pagá, T. Power system analysis using space-vector transformation. *Power Syst. IEEE Trans.* **2002**, *17*, 957–965. [CrossRef]

144. Shafiullah, M.; Abido, M.A. A review on distribution grid fault location techniques. *Electr. Power Components Syst.* **2017**, *45*, 807–824. [CrossRef]
145. Shen, Y.; Abubakar, M.; Liu, H.; Hussain, F. Power quality disturbance monitoring and classification based on improved PCA and convolution neural network for wind-grid distribution systems. *Energies* **2019**, *12*, 1280. [CrossRef]
146. Flandrin, P. *Time-Frequency/Time-Scale Analysis*; Academic Press: Cambridge, MA, USA, 1998.
147. Auger, F.; Flandrin, P.; Goncalves, P.; Lemoine, O. *Time-Frequency Toolbox, for Use with Matlab*; Technical Report; CNRS, GDR ISIS: 1995–1996. Available online: http://tftb.nongnu.org/refguide.pdf (accessed on 8 August 2021).
148. Rilling, G.; Flandrin, P.; Goncalvs, P. On Empirical Mode Decomposition and its algorithms. In Proceedings of the IEEE-EURASIP Workshop on Nonlinear Signal and Image Processing NSIP-03, Grado, Italy, 20–23 June 2003.
149. Mallat, S. *A Wavelet Tour of Signal Processing: The Sparse Way*, 3rd ed.; Academic Press: Cambridge, MA, USA, 2008.
150. Jopri, M.; Abdullah, A.; Manap, M.; Yusoff, M.; Sutikno, T.; Habban, M. An improved detection and classification technique of harmonic signals in power distribution by utilizing spectrogram. *Int. J. Electr. Comput. Eng.* **2017**, *7*, 12. [CrossRef]
151. Avdakovic, S.; Nuhanovic, A.; Kusljugic, M.; Music, M. Wavelet transform applications in power system dynamics. *Electr. Power Syst. Res.* **2012**, *83*, 237–245. [CrossRef]
152. Mroczka, J.; Szmajda, M.; Górecki, K. Gabor transform, spwvd, gabor-wigner transform and wavelet transform-tools for power quality monitoring. *Metrol. Meas. Syst.* **2010**, *17*, 383–396.
153. Abdullah, A.R.B.; Sha'ameri, A.Z.B.; Jidin, A.B. Classification of power quality signals using smooth-windowed Wigner-Ville distribution. In Proceedings of the 2010 International Conference on Electrical Machines and Systems, Incheon, Korea, 10–13 October 2010; pp. 1981–1985.
154. Cohen, L. Time-frequency Distributions: A Review. *Proc. IEEE* **1989**, *77*, 941–981. [CrossRef]
155. Auger, F.; Flandrin, P. Improving the readability of time-frequency and time-scale representations by the reassignment method. *IEEE Trans. Signal Process.* **1995**, *43*, 1068–1089. [CrossRef]
156. Camarena-Martinez, D.; Valtierra-Rodriguez, M.; Perez-Ramlu2005empiricalirez, C.A.; Amezquita-Sanchez, J.P.; de Jesus Romero-Troncoso, R.; Garcia-Perez, A. Novel downsampling empirical mode decomposition approach for power quality analysis. *IEEE Trans. Ind. Electron.* **2015**, *63*, 2369–2378. [CrossRef]
157. Lu, Z.; Smith, J.; Wu, Q.; Fitch, J. Empirical mode decomposition for power quality monitoring. In Proceedings of the 2005 IEEE/PES Transmission & Distribution Conference & Exposition: Asia and Pacific, Dalian, China, 18 August 2005; pp. 1–5.
158. Huang, N.; Shen, Z.; Long, S.; Wu, M.; Shih, H.; Zheng, Q.; Yen, N.; Tung, C.; Liu, H. The empirical mode decomposition and Hilbert spectrum for nonlinear and nonstationary time series analysis. *Proc. R. Soc. Lond.* **1998**, *454*, 903–995. [CrossRef]
159. Amirat, Y.; Benbouzid, M.; Wang, T.; Turri, S. An ensemble empirical mode decomposition approach for voltage sag detection in a smart grid context. *Int. Rev. Electr. Eng.* **2013**, *8*, 1503–1508.
160. Ozgonenel, O.; Yalcin, T.; Guney, I.; Kurt, U. A new classification for power quality events in distribution systems. *Electr. Power Syst. Res.* **2013**, *95*, 192–199. [CrossRef]
161. Achlerkar, P.D.; Samantaray, S.R.; Manikandan, M.S. Variational mode decomposition and decision tree based detection and classification of power quality disturbances in grid-connected distributed generation system. *IEEE Trans. Smart Grid* **2016**, *9*, 3122–3132. [CrossRef]
162. Sahani, M.; Dash, P.; Samal, D. A real-time power quality events recognition using variational mode decomposition and online-sequential extreme learning machine. *Measurement* **2020**, *157*, 107597. [CrossRef]
163. Dragomiretskiy, K.; Zosso, D. Variational mode decomposition. *IEEE Trans. Signal Process.* **2013**, *62*, 531–544. [CrossRef]
164. Sahani, M.; Dash, P. Variational mode decomposition and weighted online sequential extreme learning machine for power quality event patterns recognition. *Neurocomputing* **2018**, *310*, 10–27. [CrossRef]
165. Zhao, C.; Li, K.; Li, Y.; Wang, L.; Luo, Y.; Xu, X.; Ding, X.; Meng, Q. Novel method based on variational mode decomposition and a random discriminative projection extreme learning machine for multiple power quality disturbance recognition. *IEEE Trans. Ind. Inform.* **2018**, *15*, 2915–2926. [CrossRef]
166. Wu, Z.; Huang, N.E. Ensemble empirical mode decomposition: A noise-assisted data analysis method. *Adv. Adapt. Data Anal.* **2009**, *1*, 1–41. [CrossRef]
167. Choqueuse, V.; Granjon, P.; Belouchrani, A.; Auger, F.; Benbouzid, M. Monitoring of three-phase signals based on singular-value decomposition. *IEEE Trans. Smart Grid* **2019**, *10*, 6156–6166. [CrossRef]
168. Chouhy Leborgne, R. *Voltage Sags Characterisation and Estimation*; ProQuest Chalmers Tekniska Hogskola, Dissertations Publishing: Gothenburg, Sweden, 2005.
169. Phadke, A.G.; Thorp, J.S. *Synchronized Phasor Measurements and Their Applications*; Springer: Cham, Switzerland; New York, NY, USA, 2008; Volume 1.
170. Zjavka, L. Power quality multi-step predictions with the gradually increasing selected input parameters using machine-learning and regression. *Sustain. Energy Grids Netw.* **2021**, *26*, 100442. [CrossRef]
171. Theodoridis, S.; Koutroumbas, K. *Pattern Recognition*; Elsevier Academic Press: Cambridge, MA, USA, 2003.
172. Rahul; Choudhary, B. An Advanced Genetic Algorithm with Improved Support Vector Machine for Multi-Class Classification of Real Power Quality Events. *Electr. Power Syst. Res.* **2021**, *191*, 106879. [CrossRef]
173. Karasu, S.; Saraç, Z. Investigation of power quality disturbances by using 2D discrete orthonormal S-transform, machine learning and multi-objective evolutionary algorithms. *Swarm Evol. Comput.* **2019**, *44*, 1060–1072. [CrossRef]

174. Motlagh, S.Z.; Foroud, A.A. Power quality disturbances recognition using adaptive chirp mode pursuit and grasshopper optimized support vector machines. *Measurement* **2021**, *168*, 108461. [CrossRef]
175. Nagata, E.A.; Ferreira, D.D.; Bollen, M.H.; Barbosa, B.H.; Ribeiro, E.G.; Duque, C.A.; Ribeiro, P.F. Real-time voltage sag detection and classification for power quality diagnostics. *Measurement* **2020**, *164*, 108097. [CrossRef]
176. Baghaee, H.R.; Mlakić, D.; Nikolovski, S.; Dragicević, T. Support vector machine-based islanding and grid fault detection in active distribution networks. *IEEE J. Emerg. Sel. Top. Power Electron.* **2019**, *8*, 2385–2403. [CrossRef]
177. Kandel, A. *Fuzzy Expert Systems*; CRC Press: Boca Raton, FL, USA, 1991.
178. Liao, Y.; Lee, J.B. A fuzzy-expert system for classifying power quality disturbances. *Int. J. Electr. Power Energy Syst.* **2004**, *26*, 199–205. [CrossRef]
179. Dash, P.; Mishra, S.; Salama, M.; Liew, A. Classification of power system disturbances using a fuzzy expert system and a Fourier linear combiner. *IEEE Trans. Power Deliv.* **2000**, *15*, 472–477. [CrossRef]
180. Reaz, M.B.I.; Choong, F.; Sulaiman, M.S.; Mohd-Yasin, F.; Kamada, M. Expert system for power quality disturbance classifier. *IEEE Trans. Power Deliv.* **2007**, *22*, 1979–1988. [CrossRef]
181. Abdelsalam, A.A.; Eldesouky, A.A.; Sallam, A.A. Characterization of power quality disturbances using hybrid technique of linear Kalman filter and fuzzy-expert system. *Electr. Power Syst. Res.* **2012**, *83*, 41–50. [CrossRef]
182. Biswal, M.; Dash, P.K. Measurement and classification of simultaneous power signal patterns with an S-transform variant and fuzzy decision tree. *IEEE Trans. Ind. Inform.* **2012**, *9*, 1819–1827. [CrossRef]
183. Pires, V.F.; Amaral, T.G.; Martins, J.F. Power quality disturbances classification using the 3-D space representation and PCA based neuro-fuzzy approach. *Expert Syst. Appl.* **2011**, *38*, 11911–11917. [CrossRef]
184. Styvaktakis, E.; Bollen, M.H.; Gu, I.Y. Expert system for classification and analysis of power system events. *IEEE Trans. Power Deliv.* **2002**, *17*, 423–428. [CrossRef]
185. Wang, S.; Chen, H. A novel deep learning method for the classification of power quality disturbances using deep convolutional neural network. *Appl. Energy* **2019**, *235*, 1126–1140. [CrossRef]
186. Gonzalez-Abreu, A.D.; Delgado-Prieto, M.; Osornio-Rios, R.A.; Saucedo-Dorantes, J.J.; Romero-Troncoso, R.D.J. A Novel Deep Learning-Based Diagnosis Method Applied to Power Quality Disturbances. *Energies* **2021**, *14*, 2839. [CrossRef]
187. Liu, H.; Hussain, F.; Shen, Y.; Arif, S.; Nazir, A.; Abubakar, M. Complex power quality disturbances classification via curvelet transform and deep learning. *Electr. Power Syst. Res.* **2018**, *163*, 1–9. [CrossRef]
188. Ma, J.; Zhang, J.; Xiao, L.; Chen, K.; Wu, J. Classification of power quality disturbances via deep learning. *IETE Tech. Rev.* **2017**, *34*, 408–415. [CrossRef]
189. Xiao, F.; Lu, T.; Wu, M.; Ai, Q. Maximal overlap discrete wavelet transform and deep learning for robust denoising and detection of power quality disturbance. *IET Gener. Transm. Distrib.* **2020**, *14*, 140–147. [CrossRef]
190. Balouji, E.; Salor, O. Classification of power quality events using deep learning on event images. In Proceedings of the 2017 3rd International Conference on Pattern Recognition and Image Analysis (IPRIA), Shahrekord, Iran, 19–20 April 2017; pp. 216–221.
191. Varga, E.D.; Beretka, S.F.; Noce, C.; Sapienza, G. Robust real-time load profile encoding and classification framework for efficient power systems operation. *IEEE Trans. Power Syst.* **2014**, *30*, 1897–1904. [CrossRef]
192. Claessens, B.J.; Vrancx, P.; Ruelens, F. Convolutional neural networks for automatic state-time feature extraction in reinforcement learning applied to residential load control. *IEEE Trans. Smart Grid* **2016**, *9*, 3259–3269. [CrossRef]
193. Liao, H.; Milanović, J.V.; Rodrigues, M.; Shenfield, A. Voltage sag estimation in sparsely monitored power systems based on deep learning and system area mapping. *IEEE Trans. Power Deliv.* **2018**, *33*, 3162–3172. [CrossRef]